5-2005

Polyampholyte Hydrogel Characteristics and Detecting the Bacterial Interactions With These Hydrogels Using Digital Image Processing Methods

Ram Pratap Gangadharan
University of Tennessee - Knoxville

To the Graduate Council:

I am submitting herewith a thesis written by Ram Pratap Gangadharan entitled "Polyampholyte Hydrogel Characteristics and Detecting the Bacterial Interactions With These Hydrogels Using Digital Image Processing Methods." I have examined the final electronic copy of this thesis for form and content and recommend that it be accepted in partial fulfillment of the requirements for the degree of Master of Science, with a major in Engineering Science.

A.E.English, Major Professor

We have read this thesis and recommend its acceptance:

Mohamed Mahfouz, Mehran Kasra

Accepted for the Council:
Carolyn R. Hodges

Vice Provost and Dean of the Graduate School

(Original signatures are on file with official student records.)

To the Graduate Council:

I am submitting herewith a thesis written by Ram Pratap Gangadharan entitled, "Polyampholyte Hydrogel characteristics and detecting the bacterial interactions with these hydrogels using digital image processing methods". I have examined the final electronic copy of this thesis for form and content and recommend that it be accepted in partial fulfillment of the requirements for the degree of Master of Science, with a major in Engineering Science.

A.E.English
Major Professor

We have read this thesis
and recommend its acceptance:

Mohamed Mahfouz

Mehran Kasra

Accepted for the Council:

Anne Mayhew
Vice Chancellor
and Dean of Graduate Studies

(Original signatures are on file with official student records)

POLYAMPHOLYTE HYDROGEL CHARACTERISTICS AND DETECTING THE BACTERIAL INTERACTIONS WITH THESE HYDROGELS USING DIGITAL IMAGE PROCESSING METHODS

A Thesis

Presented for the

Master of Science Degree

The University of Tennessee, Knoxville

Ram Pratap Gangadharan

May 2005

DEDICATION

I dedicate this thesis to my mom, dad, sister and brother for their love and encouragement. I am grateful to all my friends both here in the US and back home in India. I owe it all to you.

ACKNOWLEDGEMENTS

Sincere thanks to my advisor Assistant Professor Dr. A.E.English for providing me the opportunity to pursue my Master's at this university and for guiding me towards the completion of this thesis. I also thank Dr. Mohamed Mahfouz for his kind cooperation in the image processing part of this thesis and Dr. Mehran Kasra for his flexibility, support, and willingness to help and serve on my thesis committee. Also this work was supported in part by American Heart Foundation and National Science Foundation. Thanks to the entire faculty and staff at our department for making my graduate studies such a rewarding experience.

ABSTRACT

In recent years, the unique physical properties of synthetic hydrogels have been exploited in a number of interesting and novel applications. In particular polyampholytes have been the subject of many theoretical studies since they provide a model for studying the long-range interactions found in proteins and other forms of soft condensed matter. In balanced polyampholytes the net electrostatic forces are attractive so that in low ionic salt concentration, the chains have a tendency to collapse into compact globules. Addition of salt, which screens these interactions, induces a swelling of the chain. However the electrostatic interactions between polymeric and mobile charges that determine the hydrogel swelling equilibrium at high ionic strengths are still not very well understood. The purpose of this Master's thesis is to analyze the characteristics of balanced polyampholytes with different charge offsets produced by systematically varying the relative proportions of 2-sulfoethyl methacrylate -2-methacryloxyethyltrimethyl ammonium chloride (SEMA-MAETAC) in copolymers of 2-hydroxyethyl methacrylate (HEMA). Hydrogel equilibrium swelling measurements were made in different bath solutions such as DI (de-ionized) water, PBS (phosphate buffer solution) and different Nacl concentration. A slight swelling in DI water and collapse transitions at intermediate salt concentrations observed experimentally provides the equivalent results, compared with the earlier studies done on balanced polyampholytes. However the deswelling of the hydrogels in high ionic salt concentration found to be abnormal. Hydrogel membrane potential has been measured using a novel method considering the Donnan potential and the Diffusion potential at a charged membrane/salt solution interface. For the balanced polyampholyte hydrogel charges ranging from 0mM to 160mM we observe a negative

slope in the steady state potential whereas we observe a positive slope in the steady state potential for the highest charged balanced polyampholyte hydrogel, which is 200mM in this case. Finally digital image processing techniques have been applied to examine the bacteria *Pseudomonas fluorescens 5RL* and hydrogel interactions. And the higher proliferation rates of the bacteria *Pseudomonas fluorescens 5RL* over neutral HEMA hydrogels compared to copolymer HEMA hydrogels with balanced charge densities in the range of 40 mM to 160 mM were analyzed using these techniques. Comparative change in the micro motion of the bacteria over balanced polyampholyte hydrogels and the unbalanced polyelectrolyte hydrogels were also presented. The cumulative result of this thesis is that the selection of the acidic and basic monomers used in the preparation of these hydrogels and their micro structural arrangements should be given importance and also the emphasis of digital image processing techniques in the application of molecular imaging.

TABLE OF CONTENTS

LIST OF TABLES

LIST OF FIGURES

CHAPTER 1: INTRODUCTION

I.INTRODUCTION

A.WHAT ARE HYDROGELS?

Hydrogel refer to certain materials that are able to swell under conditions of excess water and hold a large amount of water in the wet state. Hydrogel polymers have exceptional promises for Bio-medical use and are characterized by the pronounced affinity of their chemical structures for aqueous solutions in which they swell rather than dissolve. Hydrogels generally consist of three-dimensional polymer networks (**Figure A3-1**), which are cross-linked chemically and/or physically. The chemical properties of hydrogels are determined by the polymer backbone, the functional side chain in the monomer unit, and the cross-linking agent. The physical properties—for example, mechanical strength and swelling ratio—are controlled by the cross-link density [1]. Hydrogels can be classified based on the preparation method as homopolymer hydrogels (one type of hydrophilic mer), copolymer hydrogels (two types of mer, at least one is hydrophilic), multipolymer hydrogels (more than three types of mers). Hydrogels can also be classified based on ionic charges as neutral hydrogels, anionic hydrogels, cationic hydrogels, and ampholytic hydrogels.

B.APPLICATION OF HYDROGELS

In recent years, the unique physical properties of synthetic hydrogels and their capacity to contain a large volume of solvent in their swollen state, they have been used in a variety of interesting and novel applications. Hydrogel polymers are hydrophilic resins that

display excellent biocompatibility, which has allowed their application in diverse fields of surgery and medicine. Wichterle and Lim developed the original hydrogel polymer, a copolymer of 2-hydroxyethyl methacrylate and ethylene dimethacrylate, in 1954. The development of the first soft hydrogel contact lenses by Wichterle in 1961 represented the first successful clinical application of hydrogel polymers and remains one of the most important uses of hydrogels today. The biocompatibility of hydrogel polymers may be adapted to diverse tissue types by small variations in the makeup of the polymer, including varying the type and amount of monomers and differing the amounts and characteristics of the cross-linking agents used to create the polymer chains [2]. Biomaterials and biomedical engineering practices involve drug delivery carriers, tissue engineering scaffolds, and biomedical devices. Hydrogels provide adequate materials for these purposes. The research area of biomaterials is a multidisciplinary field composed of materials science, chemical engineering, medical engineering, and pharmacology. In particular, a biomaterial can play an important role as a bio-matrix and a bio-interface. Hydrogels provide excellent properties for improving conventional biomaterials, using such elements as copolymerization and polymer blends. As drug carriers, hydrogels can achieve stimuli-responsive drug release (for example, using pH or temperature) synchronized with enzymatic or non-enzymatic degradation. Hydrogels may be loaded with a variety of drugs and solubilizers or excipients. One major advantage of using hydrogels as a three-dimensional tissue reconstruction scaffold is the ability of these highly hydrophilic cross-linked polymer networks to swell and absorb sufficient amounts of cell culture medium [1]. The permeability of the medium is important to the exchange of water-soluble molecules such as nutrients and gases. Widely used hydrogel medical

devices include not only disposable materials, such as syringes, sample bags, and sample tubes, but also artificial organs such as blood vessels. The most promising applications may involve lenses, muscle models, and artificial cartilage. Contact lenses are a major application of hydrogel products due to their high transparency [1, 3-12]. The implementation of biomaterials based on hydrogels includes dental and ophthalmic materials, elements of implants, constituents of hybrid-type organs, as well as stimuli sensitive systems [2].

C. POLYAMPHOLYTE HYDROGELS AND ITS SIGNIFICANCE

Polyampholytic hydrogels are cross-linked polymer networks that are made up of both positive and negative monomeric groups with the possible inclusion of neutral monomeric spacers. Anthony E. English *et al* [21] performed various studies with polyampholyte hydrogels to examine the equilibrium swelling properties of polyampholyte hydrogels and also to analyze the role of counter ions shielding and ion dissociation equilibria in polyampholytic hydrogels near their balance point where both polyelectrolyte and polyampholyte effects are present. The potential use of polyampholyte hydrogels in various novel applications are dependent on the physical and the mechanical properties of these hydrogels .The study of polyampholyte polymers is at the boundary between polymer physics and biophysics. From the polymer point of view, polyampholytes are challenging heteropolymers with properties that are very different from those of conventional polyelectrolyte polymers, which contain monomers of only one charge sign. From the biophysical perspective, the presence of both positively and

negatively charged groups in a quenched sequence and the possibility for undergoing a coil-globule transition make the polyampholytes useful as simplified models for the study of protein folding [13-15]. Polyampholytes have been the subject of many theoretical studies since they provide a model for studying the long-range interactions found in proteins and other forms of salt condensed matter [16-20]. Balanced polyampholytes have an equal number of positive and negative charges while unbalanced polyampholytes have charge excess. The long-range Coulombic interactions, which determine the physical properties of polyampholytes, are a challenge to both theoretical and experimental understanding [21]. In balanced polyampholytes the net electrostatic forces are attractive so that, in pure water, the chains have a tendency to collapse into compact globules. Addition of salt, which screens these interactions and weakens the intrachains, induces a swelling of the chain [22]. Polyampholytes have been the subject for many studies focusing essentially on their swelling behavior [21, 23-29]. Balanced polyampholytes hydrogels collapse in low ionic strength conditions and swell at high salt concentration. When the net charge is increased, polyelectrolyte behavior is observed and the equilibrium swelling degree decreases with increasing salt concentration. For polyampholytes near the balance point, polyelectrolyte effect is dominant at low salt concentration, whereas the polyampholyte behavior appears at high salt concentration. To promote a specific cell-receptor interaction, these hydrogels may be modified in the bulk with cell adhesion specific peptide ligands. However, todate, the surface concentrations of these bulk-modified hydrogels have only been estimated [30-34].

II. MOTIVATION/PROBLEM DEFINITION

There is a growing interest in developing engineered actuation systems that have properties more in common with soft biological materials, such as muscles and tendons, than with traditional engineering materials. As in an aqueous environment, hydrogels will undergo a reversible phase transformation that results in dramatic volumetric swelling and shrinking upon exposure and removal of a stimulus. Thus these materials can be used as muscle-like actuators, fluid pumps and valves [8, 35, 36].

Moreover, recently it has become intensively necessary to analyze the ion transport phenomena precisely in aqueous, organic, electrolyte solution systems across a membrane from the standpoint of industrial and medical applications. Nowadays ion exchange membranes are used successfully for diffusion dialysis, ion-exchange dialysis, facilitated diffusion technique based on chemical reactions of solutes with functional groups of a polymer, and reaction diffusion counter transport. It is also very interesting to know the ionic behavior across a biological membrane if the organic solvent is added. A neutral membrane separates solutes according to the differences in their size and/or in their interaction with the membrane. In addition to this, a charged membrane can separate charged solutes according to the charge of the membrane. The measure of membrane potential is a significant method for characterizing transport phenomena across a charged membrane [37, 38]. The ion-exchange membranes and application in diverse processes (electro dialysis, diffusion dialysis, reverse osmosis, membrane electrolysis, membrane fuel cells) which are energy-, resource- and environment saving. The development of ion-exchange membranes of high chemical, mechanical and thermal stability, which meet

growing demands of the aforementioned processes, is of great importance. In harsh environments, however, the chemical stability of these membranes is unsatisfactory, and thus there is a great demand for new developments.

The use of biomaterial implants can be seriously hindered by the occurrence of bacterial infections. Bacterial adhesion to biomaterial surfaces is an essential step in the pathogenesis of these infections, however the molecular and physical interactions that govern it have not been understood in detail. Bacteria may adhere to implants, subsequently grow on the surface of the implant and excrete several metabolic products, therewith constituting a community of bacteria or biofilms. Inside biofilms, bacteria are well protected against the immune system and antibiotics and therefore infections associated with biomaterial implants are difficult to treat. Infection remains a major impediment to the long- term use of many implanted or intravascular devices. Both specific and non-specific interactions may play an important role in the ability of the cell to attach to (or to resist detachment from) the biomaterial surface. Initial bacterial attraction or repulsion to a particular biomaterial surface can be described in terms of colloidal interactions. Consequently, the force of interaction depends on physiochemical parameters such as surface-free energy and charge density [39-43]. The propensity of bacteria to adhere onto surfaces has been estimated by counting the number of bacteria that remain attached to surfaces following incubation for a specified length of time [44, 45]. Bacterial adhesion and biofilm formation have applications in a number of engineering, scientific, and medical disciplines.

III. THESIS OUTLINE

This thesis presents a study to enhance our current understanding on the physical properties as well as on the theoretical models that describes the various physical processes in the balanced polyampholyte hydrogels. This is accomplished with the phase transition and swelling properties of the balanced polyampholyte hydrogels, and the characterization of surface properties of hydrogel membranes by membrane diffusion potential. The remainder of this thesis includes the application of digital image processing techniques to examine the proliferation and micro motion of bacteria over the balanced polyampholyte hydrogel surfaces to understand closely about the bacterial-biomaterial interactions and the overall conclusions of the thesis. There is an abstract, introduction, body, and conclusion to each part, so that each may be mostly inclusive.

Chapter 2, on phase transition and swelling properties of the balanced polyampholyte hydrogels, deals with the mechanical properties which includes the structure, phase transition and swelling of the hydrogels with the necessary thermodynamic property explained. This chapter will give the idea about the behavior of neutral polyampholyte hydrogels (pure HEMA) and the balanced polyampholyte hydrogels (HEMA and SEMA + MEATAC) and the subsequent swelling data of these hydrogels over De-Ionized (DI) water, Phosphate buffer solution (PBS), and different concentration of NACL salt solution are obtained.

Chapter 3, on membrane diffusion potential measurement, deals with the electrochemical potential produced on the interface between two solutions with different ion concentrations. Its magnitude is determined by the concentration ratio and the transference numbers of the ions involved. The potential difference can be measured as a function of the concentration at semi-permeable and ion-selective membranes. The

Donnan potential and the Diffusion potential governing the total membrane potential have been explained with relevant equations.

Chapter 4 discusses the application of digital image processing techniques to examine the bacterial proliferation and micro motion over the balanced polyampholyte hydrogels and compared with the micro motion of these bacteria over polyelectrolyte hydrogel surfaces which has got a number of important potential applications in biomedicine. The bacteria-biomaterial interactions are seen from the biomaterials of the low ionic charge density to the biomaterials of the high ionic charge density. In particular, this has important applications in understanding bacterial infections, living biosensor development, and bacterial-biomaterial adhesive interactions.

Finally an entire chapter is dedicated to the summary of all the conclusions of the previous chapters and a subsequent integration of those conclusions into a concise conclusion for the entire thesis.

CHAPTER 2: SWELLING MEASUREMENT AND PHASE TRANSITION OF BALANCED POLYAMPHOLYTIC HYDROGEL

ABSTRACT

The tremendous application of hydrogels in various fields had made the necessity to understand the phenomena of these materials. This study has examined the equilibrium thermodynamic properties of a series of polyampholytic hydrogels. Balanced Polyampholytes with different charge offsets were produced by systematically varying the relative proportions of 2-sulfoethyl methacrylate -2-methacryloxyethyltrimethyl ammonium chloride (SEMA-MAETAC) in copolymers of 2-hydroxyethyl methacrylate (HEMA). The monomers SEMA and MEATAC represent a strong acid and strong base therefore remain dissociated over a wide pH range. These combinations of monomers allow the production of biocompatible hydrogel substrates with very different charge and swelling states that could be used as surfaces for supporting cells. The below chapter has examined the balanced Polyampholyte hydrogels with DI water, PBS and two different Nacl concentrations. The thermodynamic property behind the swelling phenomena is also given in this paper.

I. INTRODUCTION

Hydrogels are polymer chains that are cross-linked to form a polymer network. In the presence of an aqueous solution, the polymer chains absorb water and the association, dissociation and binding of various ions to polymer chains causes the hydrogel to swell. Ionic polymer gels are composed of a solid and a liquid phase. The solid portion of the gel consists of a cross-linked polymer network with acidic or basic group bound to the

polymer chains. When immersed in a suitable solvent, the chains in the network become solvated. Crosslink's prevent complete mixing of the polymer chains and the solvent by providing an elastic restoring force that counters the expansion of the network [46]. This paper deals with the Polyampholyte hydrogels that are cross-linked polymer networks consists of both positive and negatively charged monomers. Balanced polyampholytes have an equal number of positive and negative charges while unbalanced polyampholytes have charge excess. For polyampholytes near their balance point, polyelectrolyte effect is dominant at low salt concentration, whereas the polyampholyte behavior appears at high salt concentration [47, 48]. Balanced polyampholytes collapse at low salt concentrations and swell at high salt concentrations. As the concentration of the anionic and cationic parts deviates from the equimolar ones, the swelling ratio increases rapidly. A reasonable explanation for these results is that the number of osmotically active ions in the hydrogel phase increases as the molar ratio of cationic to anionic groups diverges from unity according to the Donnan equilibrium[49]. Polyampholyte gels with a weak net charge exhibit the unique property of reaching the same degree of equilibrium swelling with widely different salt contents. This is due to screening effects, which play differently on the attractive (polyampholyte) and repulsive (polyelectrolyte) interactions [50, 51]. If the net charge is large, the chains are expected to behave like conventional polyelectrolyte in which counterions plays a major role, because they ensure the overall neutrality of the solution. For polyampholytes near their balance point both polyelectrolyte and polyampholyte effects can be important over a wide range of bath electrolyte concentration. In balanced polyampholytes the net electrostatic forces are attractive so that, in pure water, the chains have a tendency to collapse into compact globules.

Addition of salt, which screens these interactions and weakens the intrachain attractions, induces a swelling of the chain [51].

The study of polyampholyte polymers is at the boundary between polymer physics and biophysics. From the polymer point of view, polyampholytes are challenging heteropolymers with properties that are very different from those of conventional polyelectrolyte polymers, which contain monomers of only one charge sign. From the biophysical perspective, the presence of both positively and negatively charged groups in a quenched sequence and the possibility for undergoing a coil-globule transition make the polyampholytes useful as simplified models for the study of protein folding[15, 17, 18, 50]. The physical properties of polyampholytic hydrogels are a very sensitive function of their chemical composition and ambient conditions such as the pH, ion strength, and temperature. Applied mechanical forces and electric fields can also produce large changes in the macroscopic behavior of polyampholytic hydrogels. Because of their unique physical properties and physical response obtained just by varying their composition, polyampholytic hydrogels have a number of potential novel applications in engineering and medicine [52, 53] . Controlled drug delivery, absorbent materials, contact lenses, and tissue engineering applications[52, 53] have exploited the unique properties of synthetic and natural hydrogels. Understanding the interaction between composition and ambient conditions and also improving the structure of polyampholyte networks, therefore, has important implications for these applications and can yield materials with novel properties

In this study, we examine the swelling equilibrium of polyampholytic hydrogels both experimentally and theoretically and a continuum model of polyampholyte hydrogel

phase transitions based on a concise thermodynamic and geometric foundation has been developed and used to analyze the swelling pattern observed. The contribution of the dominant forces to the overall swelling response has been illustrated experimentally by systematically varying both the hydrogel and bath composition and by considering the roles of Coulombic interactions, acid dissociation, and solvent mediated effects. The non-equilibrium swelling response to changes in bath ionic strength has been interpreted in terms of competing coupled ion, diffusion reaction, polymer network mechanisms, and the potential role of film boundary effects.

II. THEORY

A. SYSTEM DEFINITION

The universe is divided into two phases: a hydrogel phase and a bath phase. The volume, temperature, and total number of particles are constants. The solvent quality in this system will be assumed a function of temperature. Solvent and ions are free to distribute themselves between these two phases and, ultimately, the limiting case where the bath phase becomes very large will be used. Since the total volume, temperature, and particle numbers are assumed constant the Helmholtz Free energy will be an extremum in equilibrium. Hence, in equilibrium the hydrogel and bath ion chemical potentials are equal, dissociation equilibrium is satisfied for the acidic and basic monomers, and osmotic swelling equilibrium is obtained.

B. FREE ENERGY MODEL

The total system free energy, ΔF^T, can be decomposed into a sum of hydrogel and bath components [51] such that

$$\Delta F^T = \Delta F^H + \Delta F^B, \tag{1.1}$$

where ΔF^H and ΔF^B represent the hydrogel and bath contributions, respectively. The hydrogel free energy is defined as [9]

$$\Delta F^H = \Delta F_{el} + \Delta F_M + \Delta F_0 + \Delta F_{ex} \tag{1.2}$$

Where ΔF_{el}, ΔF_M, and $\Delta F_{0,}$ represent the hydrogel elastic, solvent, and ionic contributions and ΔF_{ex} represent the excess free energy correction, respectively.

The Gaussian affine model for the elasticity and the solvent components of the free energy are given by the relations, [51]

$$\Delta F_{el} = \Delta F_{Fel} = \frac{3k_B T}{2}\frac{n_0 V_0}{N_x}\left[\left(\frac{n_0}{n}\right)^{\frac{2}{3}} - 1 - \frac{1}{3}\ln\left(\frac{n_0}{n}\right)\right]. \tag{1.3}$$

and

$$\Delta F_M = k_B T n_0 V_0 \left(1 - n_0 V_0\right)\left[\ln\left(1 - nv\right) + \chi nv\right], \tag{1.4}$$

where, v is the lattice site volume, n the monomer density, n_0 the reference state monomer density, V_0 the reference state polymer volume, k_B Boltzman constant, T temperature , N_x is the number of monomers between crosslink and χ is the solvent interaction parameter.

The third term in the hydrogel component of the Free energy, which represents the translational free energy of the ions in the uniform Donnan potential, is given by [51]

$$\Delta F_0 = k_B T \sum_{i=1}^{\sigma} N_i \left\{ \ln\left(\frac{N_i}{V^H} \right) - 1 \right\} + \sum_{i=1}^{\sigma} z_i e N_i \varphi , \tag{1.5}$$

where, z_i is the i[th] valance, N_i is the number of the i[th] particle in the hydrogel phase, V^H the hydrogel volume, e the unit electrostatic charge, σ is the number of ion species, and φ represents the uniform contribution to the internal potential arising from the electrostatic double layer at the hydrogel boundary.

The fourth term, which is the excess free, energy using the Debye-Huckel plus second virial coefficient, is given by [50]

$$(\Delta Fex)DHLL + B2 = -k_B TV \left[\frac{K^3}{12\pi} + \sum_{i=1}^{\sigma} \sum_{j=1}^{\sigma} c_i c_j B_{ij}(k) \right] \tag{1.6}$$

Where, k is the inverse Debye length, c_i, c_j are the concentrations of the i[th] and j[th] ions and B_{ij} is the second virial coefficient in the Mayer ionic solution.

The bath component includes the translational freedom of the bath ions and the electrostatic contribution from a uniform potential. The bath free energy for the polyampholyte system can be defined as [51]

$$\Delta F^{B} = \Delta F_{0} + \Delta F_{ex} \tag{1.7}$$

where,

$$\Delta F^{B} = k_{B}T\sum_{i=1}^{\sigma} N_{i}^{B}\left\{\ln\left(\frac{N_{i}^{B}}{V^{B}}\right)-1\right\}+\sum_{i=1}^{\sigma} z_{i}eN_{i}^{B}\varphi^{B}, \tag{1.8}$$

where the superscript indicates the corresponding bath volume, particle numbers, and uniform potential φ . Normally, the internal uniform contribution to the electrostatic potential of the hydrogel is referenced to that of the surrounding bath. The swelling equilibrium and the acidic and basic dissociation equilibrium are given in the **APPENDIX-2.**

III. METHODS AND MATERIALS

A. MONOMER SELECTION

To test the theory outlined in the previous section, polyampholyte hydrogels were prepared using the monomers 2-Hydroxyethyl methacrlate acid (HEMA), 2-sulfoethyl methacrylic acid (SEMA-H), 2-methacryloxyethyl triethylammonium chloride (MAETA-Cl), purchased from Polysciences.

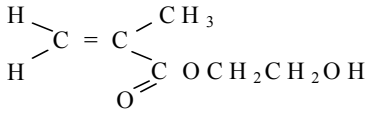

$C_6H_{10}O_3$ M.W. 130.1

2-Hydroxyethyl methacrlate acid (HEMA)

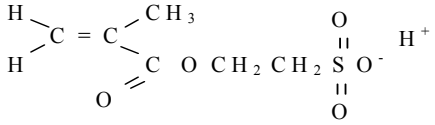

$C_6H_9O_5SH$ MW 194.1
(SEMA)

2-sulfoethyl methacrylic acid (SEMA-H)

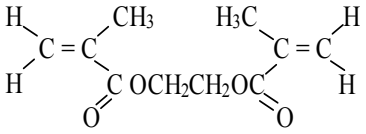

$C_{10}H_{14}O_4$ M.W. 198.22

Diethylene glycol dimethacrylate (DEGDMA)

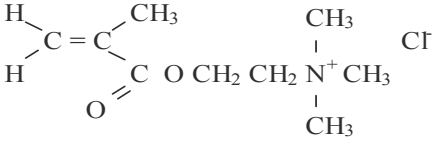

$C_9H_{18}O_2NCl$ MW 207.7
(MEATAC)

2-MethacryloxyethyltriethylammoniumChloride (MEATAC)

The above figure shows the molecular structures of HEMA, SEMA, MAETAC, and DEGDMA. Balanced Polyampholytes with different charge offsets were produced by systematically varying the relative proportions of SEMA-MAETAC in copolymers of 2-hydroxyethyl methacrylate (HEMA) where SEMA and MAETAC are strongly acidic and basic monomers. The sulfonic acid group in SEMA-H remains dissociated over a much wider pH range, making SEMA-H a much stronger acid. The strong base, MAETA-Cl, is a quaternary ammonium salt, which remains dissociated over a much wider pH range. The HEMA monomer is copolymerized with the SEMA-MAETAC monomers at their vinyl groups (CH_2=CH-).

B. HYDROGEL PREPARATION

The copolymer hydrogels were fabricated according to techniques established in this laboratory. Two molar stock solutions of the monomer HEMA, was prepared with the correct cross-linker, a 20.2 mM concentration of Diethyleneglycol dimethacrylate (DEGDMA). To prepare the SEMA-MEATAC ionic monomer stock solution, SEMA-Ag is obtained by titrating SEMA-H with Ag2co3 and then mixed with MEATAC to precipitate the Ag and Cl counterions. An aqueous solvent with 40% ethylene glycol (EG) was also used for each stock solution. The polymerization reactions were initiated with 1.76 mM ammonium persulfate (APS). The DEGDMA cross-linker, APS initiator, and EG solvent were all purchased from Aldrich Chemical Company. The solutions then were mixed in varying proportions to produce eight sets of linearly spaced copolymer hydrogels with the monomer concentrations of 0, 40, 80, 120, 160, and 200 mM. The chemical concentrations used to prepare the monomer HEMA, and the copolymer SEMA-MAETAC is shown in Table 1. A specific range of concentrations was chosen to avoid phase separation thereby making the copolymers either too brittle and hard or too soft and weak.

All hydrogel samples were degassed under a vacuum since oxygen interferes with the polymerization process. These were then saturated using nitrogen gas to help reduce the re-uptake of oxygen. After the stock solutions were degassed, the appropriate proportions of ionic stock solutions were added to aliquots of the neutral stock solutions to produce six 10 mL sample solutions with concentrations of 0, 40, 80, 120, 160, and 200 mM.

Hydrogel membranes were formed by casting several milliliters of the pregellation solution between two glass plates separated by a thin Teflon film spacer. Small metal binder clips were used to form a tight seal between the two plates. Test tubes containing the remaining solutions were each filled with several 100 μL micropipettes with inner diameters of 1293 μm. Since basic hydrogels tend to adhere to glass surfaces because of their positive charge, the micropipettes were first coated with a glass repellent consisting of a 20 g/L solution of dimethyldichlorosilane in 1,1,1-trichloroethane from Pharmicia (Repel-Silane) and washed with distilled deionized water thoroughly to remove all chemicals not affixed to the glass. These micropipettes were then blown dry and placed within the test tubes. This completed, all samples were allowed to polymerize at 25^{o}C for 24 hours.

After polymerization was complete, the hydrogels were removed from between the glass plates and placed in distilled deionized water where they were washed continuously with daily water changes for two weeks. In this way, residual non-polymerized chemicals were removed from the gels. The cylindrical hydrogels were removed from their pipettes by nicking one side of the pipette using a small glass cutter and carefully breaking and removing a small piece of gel approximately 2-3 mm in length. The gels were placed into individual glass cell holders, and washed continuously and in parallel with distilled deionized water for two weeks. This water bath was then replaced with NaCl dissolved in distilled deionized water, with a 1.54 mM concentration of NaCl solution. The gels were washed in NaCl solution for the appropriate amount of time to allow for their equilibration. After the hydrogels being washed with NaCl, it is then washed with 1× PBS (Phosphate Buffer Solution), which is taken from 10 × PBS (preparation is given in

TableA1-9). Hydrogel diameters were measured at each bath concentration using a microscope equipped with a charge coupled device camera. All diameter measurements were normalized to the inner diameter, D_0, of the cylindrical pipette in which it was cast.

IV. RESULTS AND DISCUSSION

One of the most important factors that determine the physical properties of a polyampholyte hydrogel is the relative concentration of positive and negative monomers. The charge of a monomeric group also depends on the acid and base dissociation constants. When the surrounding bath contains no ions, counterions are confined to the hydrogel phase. The electrostatic confinement of the counterions maintains charge electro neutrality and a constant total number of each type of particle. When the ions are present in the surrounding bath, it is no longer valid to define the system as a confined volume with no capacity for ion exchange. In this case, the ion chemical potentials in the bath and hydrogel phases must be equal in equilibrium. This concept is valid even for DI water having no added salt in it as even when the pH is 7 the electrostatic inclusion of hydrogen or hydroxide ions can create very low or high internal pH values, depending on the polymer charge density. Hence polyampholytes hydrogels made of very strong acidic and basic monomers can exhibit ion association effects at low salt concentration [51].

Unlike polyelectrolyte, balanced polyampholytes have the unique capacity to swell at high bath salt concentrations i.e. balanced polyampholytes collapse at low salt concentrations and swell at high salt concentrations. With increasing charge offset,

polyelectrolyte behavior is observed and swelling decreases with increasing salt concentration. The swelling response of a polyampholyte hydrogel network to changes in bath ionic strength or pH can be strongly dependent on the monomer acid and base dissociation constants. These polyampholytes have a net positive charge at low pH, a net negative charge at high pH and are neutral at some intermediate pH. Far from the isoelectric point or charge balance state, these polymers behave like polyelectrolyte and exist in a swollen state that can be forced to collapse by increasing the ionic strength. Recent experimental studies have shown that, depending on the magnitude of the net polymer charge and bath ionic strength, the swelling properties can be dominated by acid and base dissociation, electrostatic repulsion, and electrostatic attraction [21, 50, 51]. The swelling response of polyampholyte hydrogels near the balance point to changes in bath salt concentration should illustrates the competing effects of ion dissociation, polyelectrolyte screening, and polyampholyte screening. The acid and base dissociation constants play an important role in determining the background of positive and negative charges at the isoelectric point. When the difference in the dissociation constants of the acidic and basic monomers is much higher, there exist a large background of positive and the negative charges at the isoelectric point. When a significant background of charges exists at the isoelectric point, attraction between oppositively charged side chains leads to a relatively tight coiling of the polyions at low bath ionic strengths due to the ion association. The subsequent loss in charge density and the osmotic pressure therefore produces a deswelling transition at low ionic bath salt concentration. Increasing the bath salt concentration weakens the intrachain attractions and leads to the exchange of sodium ions and chloride ions in the acidic and basic monomers and hence the acidic and basic

monomers dissociate which creates the swelling transition in the hydrogels. Thus at the low ionic strengths, ion dissociation equilibrium and attractive polyampholyte effects dominate the swelling responses. At the intermediate bath ionic strengths, polyelectrolyte screening produces the deswelling transition as a result of losing the osmotic pressure difference between the hydrogel and the surrounding bath. Upon a further increase in the bath salt concentration, there is a swelling transition again because of the screening of the attractive polyampholyte interactions and excluded volume effects. Most theoretical treatments of polyampholyte swelling however have been based on the Debye-Huckel limiting law osmotic correction, but it is only valid for low ionic concentrations [54, 55]. The electrostatic interactions between polymeric and mobile charges that determine the hydrogel swelling equilibrium at high ionic strengths arte, therefore, still not a very well understood.

The results of the swelling curve for the Polyampholyte hydrogels with different bath solutions is given in the **Appendix 3** and the necessary graphs have been plotted with the resulting data. It has to be stated while taking the swelling measurement, the gel with the 80mM concentration has been missed and it has been replaced with the other one of the same 80mM concentration. Due to this the swelling of the 80mM concentration gel seems to be differing from the other gels of different concentration due to the kinetic effects. Similar to 80mM gel, the 200mM gel has been found lost and it has also been replaced with another one of the same type and the measurements are preceded. The swelling response of polyampholyte hydrogels near the balance point in DI water, 1.54mM Nacl, PBS and 1.5M Nacl is obtained and the **Table 2.1**, **Table 2.2**, **Table 2.3** shows the

Table 2.1. Hydrogel Diameter Measurements (in Pixels).

PAGEL	JAN30-04	FEB4-04	FEB5-04	FEB6-04	FEB9-04	FEB10-04	FEB11-04	FEB13-04	FEB14-04	FEB16-04	FEB23-04	FEB27-04	APR15-04
	DI H2O	DI H2O	DI H2O	DI H2O	DI H2O	DI H2O	DI H2O	DI H2O	DI H2O	DI H2O	DI H2O	DI H2O	DI H2O
(mM)	(Pix)	(Pix)	(Pix)	(Pix)	(Pix)	(Pix)	(Pix)	(Pix)	(Pix)	(Pix)	(Pix)	(Pix)	(Pix)
0	145	136	145	146	136	136	136	139	137	137	140	155	132
40	170	172	172	172	170	170	171	150	142	142	146	207	136
80	141	0.00	141	141	142	143	142	141	141	142	142	196	136
120	195	194	194	194	193	194	194	154	148	148	157	243	138
160	238	239	240	242	239	236	237	171	157	157	166	275	137
200	236	242	244	244	181	145	146	147	146	147	147	265	139

Table 2.2. Hydrogel Diameter Measurements (in Microns).

PAGEL	JAN30-04	FEB4-04	FEB5-04	FEB6-04	FEB9-04	FEB10-04	FEB11-04	FEB13-04	FEB14-04	FEB16-04	FEB23-04	FEB27-04	AP15-04
	DI H2O	DI H2O	DI H2O	DI H2O	DI H2O	DI H2O	DI H2O	DI H2O	DI H2O	DI H2O	DI H2O	DI H2O	DI H2O
(mM)	(Mic)	(Mic)	(Mic)	(Mic)	(Mic)	(Mic)	(Mic)	(Mic)	(Mic)	(Mic)	(Mic)	(Mic)	(Mic)
0	106.62	100.00	106.62	107.35	100.00	100.00	100.00	102.21	100.73	100.73	102.94	113.97	97.06
40	125.00	126.47	126.47	126.47	125.00	125.00	125.73	110.29	104.41	104.41	107.35	152.21	100.00
80	103.68	0.00	103.68	103.68	104.41	105.15	104.41	103.68	103.68	104.41	104.41	144.12	100.00
120	143.38	142.65	142.65	142.65	141.91	142.65	142.65	113.23	108.82	108.82	115.44	178.68	101.47
160	175.00	175.73	176.47	177.94	175.73	173.53	174.26	125.73	115.44	115.44	122.06	202.20	100.73
200	173.53	177.94	179.41	179.41	133.09	106.62	107.35	108.09	107.35	108.09	108.09	194.85	102.21

Table 2.3. Hydrogel Diameter Measurements (D/Do in Microns).

PAGEL	JAN30-04	FEB4-04	FEB5-04	FEB6-04	FEB9-04	FEB10-04	FEB11-04	FEB13-04	FEB14-04	FEB16-04	FEB23-04	FEB27-04	APR15-04
	DI H2O	DI H2O	DI H2O	DI H2O	DI H2O	DI H2O	DI H2O	DI H2O	DI H2O	DI H2O	DI H2O	DI H2O	DI H2O
(mM)	(Mic)	(Mic)	(Mic)	(Mic)	(Mic)	(Mic)	(Mic)	(Mic)	(Mic)	(Mic)	(Mic)	(Mic)	(Mic)
0	0.88	0.82	0.88	0.88	0.82	0.82	0.82	0.84	0.83	0.83	0.85	0.94	0.80
40	1.03	1.04	1.04	1.04	1.03	1.03	1.04	0.91	0.86	0.86	0.88	1.25	0.82
80	0.85	0.00	0.85	0.85	0.86	0.87	0.86	0.85	0.85	0.86	0.86	1.19	0.82
120	1.18	1.18	1.18	1.18	1.17	1.18	1.18	0.93	0.90	0.90	0.95	1.47	0.84
160	1.44	1.45	1.45	1.47	1.45	1.43	1.44	1.04	0.95	0.95	1.01	1.67	0.83
200	1.43	1.47	1.48	1.48	1.10	0.88	0.88	0.89	0.88	0.89	0.89	1.61	0.84

respected data obtained for the swelling response of the hydrogels for the above bath solutions and for different time periods. **Figure A3-2** shows the microscopic images of the balanced polyampholyte hydrogel with charges 0, 40, 80, 120, 160, 200 mM taken on Jan30 for the initial swelling measurement. **Figure A3-3** shows the initial swelling measurement curves of the hydrogels taken on Jan 30th of different charge concentration after washed with DI water. There is a slight swelling transition in the initial measurements of the hydrogels as seen from the graph plotted and the reason could be due to the fact that the ion chemical potentials in the bath and hydrogel phases must be equal in equilibrium even for DI water having no added salt in it, as even when the pH is 7 the electrostatic inclusion of hydrogen or hydroxide ions can create very low or high internal pH values, depending on the polymer charge density and it could cause the swelling pattern in the hydrogels. The graph of **Figure A3-5**, shows the swelling of the hydrogels which was washed until Feb 11th with DI water with no salt in it and the respective microscopic images used for the swelling measurements were given in the **Figure A3-4** and as the hydrogels are balanced Polyampholyte there is no much swelling when washed with DI water as seen in the graph plotted in **Figure A3-5**. When the hydrogels washed with 1.54mM Nacl solution, there is a deswelling pattern as shown in the **Figure A3-7**and **Figure A3-**9 for all the hydrogels which shows the polyelectrolyte screening taking effect in this cases as the bath salt concentration increases, the osmotic pressure difference between the hydrogel and the surrounding bath decreases, which results in a deswelling pattern. **Figure A3-6** and **Figure A3-8** shows the respective microscopic images used to obtain the swelling measurement for the graph obtained in

Figure A3-7 and **Figure A3-9. Figure A3-10** shows the images of the hydrogels after being washed with 1 x PBS, to check whether the hydrogels swell faster in the presence of buffered solutions as the conjugate base of the buffer reversibly binds hydrogen ions in regions of higher concentration and releases the hydrogen ion after diffusing to a region of lower concentration [56]. **Figure A3-11** provides the graph for the swelling measurement of the hydrogels for the above PBS bath solution and the graph doesn't show any difference in swelling pattern. When the hydrogels are allowed to wash in DI water again, we see a swelling pattern in the hydrogels as shown in the **Figure A3-12** due to the increase in the cations in the hydrogel phase which increases the osmotic pressure and the graph has been plotted in **Figure A3-13** using the measurements taken from **Figure A3-12**. The hydrogels are again washed with higher salt concentration i.e. 1.5M Nacl salt concentration. **Figure A3-14** and **Figure A3-15** shows the microscopic images and the graph plotted for the hydrogels in 1.5M Nacl salt concentrations. Balanced polyampholyte hydrogels are expected to swell at higher salt concentration due to the ionic dissociation, but **Figure A3-15** shows a deswelling pattern that founds to be abnormal. The reason may be due to the micro structural arrangement of charged and neutral monomers during the polymerization reaction that could have played a role in the decrease of the osmotic pressure difference between the hydrogel phase and the bath phase.

V. CONCLUSION

This chapter has discussed the preparation of a series of balanced Polyampholyte hydrogels and their corresponding thermodynamic behaviors. The phase transition of Polyampholyte hydrogels has been shown and necessary theoretical background has been provided. The swelling transition of the balanced polyampholyte hydrogels for different bath solutions is measured and the respective graphs have been plotted to examine the results. Polyampholyte hydrogels possess positive and negative charges. The acid and base dissociation constants of the monomers play an important role in determining the swelling response of the polyampholyte hydrogels to changes in the bath solutions. The results show that polyampholyte hydrogels exhibits properties similar to polyelectrolyte hydrogels and collapse at intermediate bath ionic salt concentration. But instead of swelling in the higher salt concentration our result shows that there is a deswelling pattern.

The swelling response of a polyampholyte is higher dependent on the relative concentration and micro structural arrangement of charged and neutral monomers established during polymerization. The microstructure has been shown to depend on the type of monomers used in the feedstock and the conditions under which the polymerization. Although counterions are normally present in unbalanced polyampholytes to maintain charge electroneutrality, even balanced polyampholytes can bear residual counterions. Counterions screening during polymerization normally leads to

a random monomer distribution with no preferential arrangement based on the monomer charges.

This study has given an importance in the selection of the monomers used in the preparation of these hydrogels, the micro structural arrangement of the monomeric groups during polymerization reaction and to the counterions in the hydrogel phase of the balanced Polyampholyte hydrogels, which could turn the actual property of these hydrogels. The deswelling of the balanced polyampholytic hydrogels inspite of swelling during the inclusion of high salt concentration could be due to the mentioned reason and also due to the micro structural arrangement of charged and neutral monomers during the polymerization reaction which could have played a role in the decrease of the osmotic pressure difference between the hydrogel phase and the bath phase.

CHAPTER 3: HYDROGEL MEMBRANE POTENTIAL MEASUREMENT

ABSTRACT

The origin of a membrane charge is clear. When brought into contact with an aqueous electrolyte solution, membranes do acquire an electric charge through several possible mechanisms. These mechanisms may include dissociation of functional groups, adsorption of ions from solution, and adsorption of charged macromolecules. This charging mechanism can take place as well on the exterior membrane surface as on the interior pore surface of the membrane. These surface charges have an influence on the distribution of ions in the solution due to the requirement of the electroneutrality of the system. We have developed a novel measurement method of the Donnan potential and the Diffusion potential at a charged membrane/salt solution interface. This method is useful for obtaining the effective charge density of each layer of a bipolar membrane.

I.INTRODUCTION

Flow of matter from one region to another is determined by the potential energy of the system. Movement of water across a semi permeable membrane, in the absence of a hydraulic pressure difference e.g. a column of water, can result from three kinds of potential energy: chemical potential, electrical-potential, and thermal-potential. This potential can result in a flow of solutes (dissolved chemicals), electricity and/or heat. This non-hydraulic flow is called osmosis. In an aqueous solution, an electrical potential develops where there is a separation of charge such that two regions exist, where one has a predominantly positive charge due to the accumulation of cations and one has a

predominantly negative charge due to the accumulation of anions. When a semipermiable membrane is used to separate the chambers containing two different concentrations of solutions then there arise the Nernst potential due to the concentration difference in the two chambers and the Donnan potential due to the charges in the boundary.

In this section we are going to measure the membrane potential of Polyampholyte hydrogel due to the diffusion of charges between two different concentration of NACL solution separated by the membrane and the measurement is continued with different salt concentration and also with Polyampholyte hydrogel of different charge density. The boundary potential i.e., the potential obtained due to the charges in the surface of the hydrogel is also considered along with diffusion potential obtained due to the concentration of charges. The charge of a membrane can be also reflected in the boundary potential as the charges at the pore walls play a significant role on the ions flow in the membrane [57].

II. EXPERIMENTAL THEORY

A. DIFFUSION PRINCIPLE

In solutions ions are free to move, so that eventually equilibrium is maintained and no potential is measurable between different regions in a simple solution of electrolytes. However, if NaCl solutions of different concentrations are brought together a Diffusion Potential or Liquid Junction Potential results immediately and transiently, because of the differences in the mobility's of the ions. Na+ and Cl- diffuse as separate units. Na+ moves

more slowly than Cl- and the resulting separation of the opposite charged ions establishes a potential at the boundary (junction) between the two solutions, the positive side in this case being the more concentrated solution. Generally smaller ions have higher mobility's than larger ones, and multivalent ions have a lower mobility than mono-valent ones of the same size. This is all because of differing abilities to bind water.

Difference in mobility can be attributed to the shell of hydration each type of ion has. Each ion carries an associated “cloud” of water molecules that are attracted by the charged state of the ion. In sodium (Na+) this “cloud” is larger than that found in chloride (Cl-). Thus the (Cl-) on the left side will rise faster than (Na+) and this voltage difference (or potential) is the Diffusion Potential. Ultimately this potential dissipates as equilibrium is attained. When a semipermiable membrane is used to separate the chamber of solutions of different NACL solution then we get the membrane potential which is a combination of Donnan potential resulting due to the accumulation of either positive or negative charges over the surface of the membrane, the diffusion potential due to the diffusion of charges from higher concentration to lower concentration and also the charge of the semipermiable membrane, as the concentration gradient created across the membrane, the charge at the pore walls can play a significant role on the ions flow in the membrane.

B. DONNAN POTENTIAL

There exists an electrical potential difference between two salt solutions of different concentration separated by an ion-exchange membrane, which could be the balanced polyampholyte hydrogel in this case in the absence of any current flowing through the

membrane. The concentration difference between the salt solutions will set up a diffusional force driving the sodium chloride from the higher concentration into the lower concentration through the hydrogel membrane. The chloride ions have higher diffusivity rate than sodium ions. Consequently, excess negative electrical charges will accumulate on the low concentration solution side of the membrane, while excess positive electrical charges will accumulate on the high concentration side because of the positively charged sodium cations that are left behind. This charge separation will induce an electrical potential difference that will drive the electro-migration of the chloride ions in the direction opposite to that of the diffusion. The overall result will be that the net movement of the chloride ions into the lower concentration solution will slow and eventually stop when the two opposing forces are equal and the two opposing fluxes are equal which is said to have attained the Donnan Equilibrium. The electrical potential difference across the membrane under these equilibrium conditions is the "Donnan potential".

The donnan potential, which depends on the membrane charge density, plays a very important role in the selectivity of the membrane with respect to the valance of the ions [58].

The electrochemical potentials of the i^{th} ion in the salt solution and in the polyelectrolyte hydrogel are given by μ_i and $\overline{\mu}_i$, respectively:

$$\mu_i = \mu_i^0 + RT \ln \gamma_i C_i + z_i F \phi, \qquad i=+,- \tag{3.1}$$

$$\overline{\mu}_i = \overline{\mu}_i^0 + RT \ln \overline{\gamma}_i \overline{C}_i + z_i F \overline{\phi}, \qquad i=+,- \tag{3.2}$$

where μ_i and $\overline{\mu}_i$ are the standard electrochemical potentials, z_i is the valence of the ion, R is the gas constant, T is the absolute temperature, γ_i and $\overline{\gamma}_i$ are the ion activity coefficients, C_i and $\overline{C}_i$ are the ion concentrations, F is the Faraday constant while ϕ and $\overline{\phi}$ are the electrical potentials; the bar denotes the values in the charged membrane [59].

At the interface between the membrane and the external electrolyte solution, the electrochemical potentials in the two phases are equilibrated:

$$\mu_i = \overline{\mu}_i, \quad i = +,- \tag{3.3}$$

The Donnan potential, $\Delta\phi_{Don}$ between the membrane surface and the electrolyte solution is given as [59]

$$\Delta\phi_{Don} = \overline{\phi} - \phi = -\frac{RT}{z_i F} \ln \frac{\overline{\gamma_i}\,\overline{C_i}}{k_i \gamma_i C_i}, \; i = +,- \tag{3.4}$$

where k_i is the distribution coefficient of the ion i, defined as

$$\overline{\mu}_i^{\,0} - \mu_i^{\,0} = -RT \ln k_i, \; i = +,- \tag{3.5}$$

Under the condition, $z_+ = -z_-$, the relationship between the concentrations of ions in the membrane and in the external solution can be obtained:

$$\overline{C_+}\;\overline{C_-} = \frac{\gamma_\pm^2 C_s^2}{Q^2} \tag{3.6}$$

where C_s is the electrolyte concentration in the external solution equated as $(C_+C_-)^{1/2}$

$\gamma_\pm$ is the mean activity coefficient of the electrolyte equated as $(\gamma_+\gamma_-)^{1/2}$

Q can be expressed as

$$\mathrm{Q} = \left(\frac{\overline{\gamma_+}\,\overline{\gamma_-}}{k_+ k_-} \right)^{1/2} \tag{3.7}$$

On the other hand, the condition of electro neutrality in the membrane is given by

$$\sum_{i=+,-} z_i \overline{C_i} + z_x C_x = 0 \tag{3.8}$$

where z_x is the valence of fixed charge groups, and C_x is the fixed charge density.

$$\overline{C_+} = \sqrt{\left(\frac{z_x C_x}{2z_+}\right)^2 + \left(\frac{\gamma_\pm C_s}{Q}\right)^2} - \frac{z_x C_x}{2z_+} \tag{3.9}$$

$$\overline{C_-} = \sqrt{\left(\frac{z_x C_x}{2z_+}\right)^2 + \left(\frac{\gamma_\pm C_s}{Q}\right)^2} + \frac{z_x C_x}{2z_+} \tag{3.10}$$

The most important point in Eqs. (3.9) and (3.10) is that the mean activity coefficient of electrolytes in the external, aqueous, organic solution, $\gamma_\pm$ is multiplied to the electrolyte concentration, C_s. The effect of mean activity coefficient of the electrolyte is usually neglected in aqueous solution. Donnan potential at the left- and right-hand sides of the interface between the membrane and the surrounding solution are given by inserting Eq. (3.9) into Eq. (3.4). If it is assumed that the activity coefficients of ions are not the function of the ion concentrations in the membrane [60], the total Donnan potential through the membrane can be expressed by the sum of the Donnan potentials at the left- and right-hand sides for an aqueous, organic solution system cited above:

$$\Delta\phi_{Don(l\to r)} = -\frac{RT}{z_+ F} \ln\left[\frac{\gamma_+^{''} C_s^{''} \overline{C_+^{'}}}{\gamma_+^{'} C_s^{'} \overline{C_+^{''}}}\right] \tag{3.11}$$

where $C_s^{'}$ and $C_s^{''}$ are the concentrations of the solution in left- and right-hand sides, and $\overline{C_+^{'}}$ and $\overline{C_+^{''}}$ are the cation concentrations at the left- and right-hand sides of the charged

membrane, which are given by Eq. (9). The value of $\gamma_{+}^{''}/\gamma_{+}^{'}$ cannot be obtained singly, thus we approach it by $\gamma_{\pm}^{''}/\gamma_{\pm}^{'}$ and will not make obvious errors. Therefore the above equation becomes

$$\Delta\phi_{Don(l\to r)} = -\frac{RT}{z_{+}F}\ln\left[\frac{\gamma_{\pm}^{''}C_{s}^{''}\overline{C_{+}^{'}}}{\gamma_{\pm}^{'}C_{s}^{'}\overline{C_{+}^{''}}}\right] \tag{3.12}$$

C. MEMBRANE DIFFUSION POTENTIAL

There is a potential developed due to the diffusion of ions from higher concentration to lower concentration we call such voltage difference as diffusion potentials because they are generated by selective ion diffusion. The diffusion potential depends on the ionic mobility in the membrane and affects the transport of ions in the membrane. The voltage difference established between the two compartments is thus a direct result of the *selective* diffusion of ions across the membrane. The membrane potential becomes more negative as more cations diffuse from left to right, and the voltage in turn limits their outward diffusion. At some point the tendency of a cation to diffuse down its concentration gradient is balanced by its equal tendency to move in the opposite direction "down" the electrical gradient. This balance of electrical and diffusion tendencies creates an electrochemical equilibrium between the opposing chemical or concentration and electrical forces. (Consequently, diffusion potentials are also often called Nernst potentials after the scientist who formally characterized the electrochemical equilibrium.)

Over time, about the same number of cations diffuses into the outside compartment as diffuse in the opposite direction, and no additional membrane potential develops.

The ionic flux across the membrane is given by the Nernst-Planck equation, which can be applied to the phase of the membrane [59]:

$$J_i = -\overline{\omega}_i RT\frac{d\overline{C}_i}{dx} - z_i F\overline{\omega}_i\overline{C}_i\frac{d\overline{\phi}}{dx}, \quad i=+,- \tag{3.13}$$

where $\overline{\omega}_i$ is the ionic mobility of the ion i in the membrane. The electro-neutrality condition in a membrane requires that

$$J_+(x) = J_-(x) \tag{3.14}$$

Differentiating hydrogel concentration terms used earlier,

$$\frac{d\overline{C}_+}{dx} = \frac{d\overline{C}_-}{dx} \tag{3.15}$$

Now after substitutions the diffusion potential can be expressed as [59]

$$\Delta\phi_{diff} = \overline{\phi}'' - \overline{\phi}' = -\frac{RT}{z_+F}\frac{r-1}{r+1}\times\ln\left[\frac{(r+1)\overline{C}_+'' + (z_x/z_+)C_x}{(r+1)\overline{C}_+' + (z_x/z_+)C_x}\right] \tag{3.16}$$

where r is the cation-to-anion mobility ratio in the membrane defined as

$$r = \frac{\overline{\omega}_+}{\overline{\omega}_-} \tag{3.17}$$

where $\overline{\omega}_+$ and $\overline{\omega}_-$ are the cation and anion mobility in the membrane, respectively.

D. MEMBRANE POTENTIAL

The membrane potential $\Delta\phi$ is the sum of the Donnan and the membrane diffusion potentials, which are given by Eqs. (3.12) and (3.16), respectively [59]

$$\Delta\phi = \Delta\phi_{Don(l\to r)} + \Delta\phi_{diff} \tag{3.18}$$

Thus Eq. (3.18) gives the total membrane potential of the hydrogel.

The **Figure A3-16** shows the hydrogel diffusion potential measurement obtained from the simulations performed with the above membrane diffusion potential equations. It has been shown that the hydrogels made out of the negative charges (blue colored points) follow a negative slope whereas the hydrogels made of positive charges (red colored points) follow a positive slope.

III. MATERIALS AND METHODS

A. MATERIALS NEEDED

The membranes studied in the present section are polyampholyte hydrogel membranes that contain the monomer of two signs i.e., both positive and negative charges. Balanced Polyampholytes with different charge offsets were produced by systematically varying the relative proportions of SEMA-MAETAC in copolymers of 2-hydroxyethyl methacrylate (HEMA) where SEMA and MAETAC are strongly acidic and basic monomers. The equipment used for this experiment to measure the steady state potential

is the EVC-4000 Multi-Channel Voltage/Current Clamp instrument, a four-channel Voltage/Current clamp apparatus which employs the voltage clamp technique to monitor membrane permeability as a function of membrane voltage or applied chemicals.

B. EXPERIMENTAL PROCEDURES

Assemble the Balanced Polyampholyte hydrogel in the membrane test chamber. Two voltage electrodes, one on either side of where the membrane is normally located are inserted into the appropriate ports on the chamber. Two current electrodes are also connected at the ports located at each distal end of their respective chambers. Note that '1' electrodes, i.e., V1 and I1 are connected on the same chamber half; similarly for '2' chamber electrodes, V2 and I2. Keep the first chamber with electrolyte (Nacl solution) in which the electrolyte concentration is often changed starting from 1.54mM, 4.87mM, 15.4mM, 48.7mM, 154mM, 487mM, 1.54M. And keep the second chamber to be a fixed one with concentration 154mM for every change in the concentration in the first chamber. Before starting the experiment set the Electrode Offset Adj. controls on the preamplifier so as to reduce the asymmetry potential to 0.00mV by keeping the concentration of electrolyte on both the chambers to be 154mM.

A series of Balanced Polyampholyte hydrogel with the charges 0mM, 40mM, 80mM, 120mM, 160mM, 200mM. is used as the membranes separating the two chambers. To start the experiment, keep the 0mM charged Polyampholyte hydrogel in between the two chambers and fill the first chamber with 1.54mM Nacl solution and the second chamber, the constant 154mM.Then the experiment is continued by keeping the 0mM membrane

and changing the Nacl concentration starting from 1.54mM to 1.54M. Similarly the experiment is done with the various charges of the Polyampholyte hydrogel membrane and carried with the same way as the experiment is done with 0mM Polyampholyte hydrogel membrane. And the results in terms of voltage are tabulated and then the results are plotted.

IV. RESULTS AND DISCUSSION

The measured values show an interesting result in the **TABLE 3.1, TABLE 3.2, TABLE 3.3, TABLE 3.4, TABLE 3.5, and TABLE 3.6,** for balanced polyampholytic hydrogels with the charges 0mM, 40mM, 80mM, 120mM, 160mM and 200mM respectively. In **Figure A3-17, Figure A3-18, Figure A3-19, Figure A3-20, Figure A3-21,** the measured voltage for the hydrogel with charges 0mM, 40mM, 80mM, 120mM and 160mM respectively, is found to be following the same pattern as the membrane potential goes through a minimum as the electrolyte concentration increases, and following a negative slope with the increase in the Nacl salt concentration. This result shows that the hydrogel membrane between the two chambers may acts like an anion exchange membrane, even though the hydrogel is a balanced polyampholyte hydrogel. We can also note from the results that the initial voltage obtained for all the hydrogel charges during the measurement is found to be decreasing with increase in the hydrogel charges. This may be due to the reduced flow of charges in the Nacl solution from one chamber to another with increase in the membrane charge in between the two chambers. When we examine

TABLE 3.1. 0Mm PA Hydrogel Concentration.

serial no	NACL SALT Concentration	Log_{10} (C1/C2)	Voltage measured
1	1.54	-2.00	25.4
2	4.87	-1.50	15.7
3	15.4	-1.00	10.1
4	48.7	-0.50	4.4
5	154	0.00	0.3
6	487	0.50	-0.2
7	1540	1.00	-0.3

TABLE 3.2. 40Mm PA Hydrogel Concentration.

serial no	NACL SALT Concentration	Log_{10} (C1/C2)	Voltage measured
1	1.54	-2.00	20.4
2	4.87	-1.50	14.8
3	15.4	-1.00	9.9
4	48.7	-0.50	2.8
5	154	0.00	0.3
6	487	0.50	0.2
7	1540	1.00	-0.2

TABLE 3.3. 80Mm PA Hydrogel Concentration.

serial no	NACL SALT Concentration	Log_{10} (C1/C2)	Voltage measured
1	1.54	-2.00	16.9
2	4.87	-1.50	10.4
3	15.4	-1.00	6.8
4	48.7	-0.50	1.5
5	154	0.00	0.3
6	487	0.50	-0.2
7	1540	1.00	-0.4

TABLE 3.4. 120Mm PA Hydrogel Concentration.

serial no	NACL SALT Concentration	Log_{10} (C1/C2)	Voltage measured
1	1.54	-2.00	13.5
2	4.87	-1.50	8.2
3	15.4	-1.00	4.6
4	48.7	-0.50	0.9
5	154	0.00	0.2
6	487	0.50	0.2
7	1540	1.00	-0.2

TABLE 3.5. 160Mm PA Hydrogel Concentration.

serial no	NACL SALT Concentration	Log_{10} (C1/C2)	Voltage measured
1	1.54	-2.00	12.2
2	4.87	-1.50	6.6
3	15.4	-1.00	4.6
4	48.7	-0.50	0.5
5	154	0.00	-0.1
6	487	0.50	-0.2
7	1540	1.00	-0.4

TABLE 3.6. 200Mm PA Hydrogel Concentration.

serial no	NACL SALT Concentration	Log_{10} (C1/C2)	Voltage measured
1	1.54	-2.00	-5.2
2	4.87	-1.50	-4.8
3	15.4	-1.00	-1.5
4	48.7	-0.50	-0.6
5	154	0.00	0
6	487	0.50	0.2
7	1540	1.00	0.3

the result of 200mM Polyampholyte hydrogel as shown in the graph plotted in the **Figure A3-21**, the membrane potential goes through a maximum as the electrolyte concentration increases and follows a positive slope. The reason for this change in the slope from negative to positive could be due to the membrane charge density, which is higher when compared to the remaining charged hydrogels. This result also gives an idea that the hydrogel membrane in between the two chambers may acts like a cation exchange membrane, even though the hydrogel is a balanced Polyampholyte hydrogel.

V. CONCLUSION

This experimental study about the membrane potential of the balanaced polyampholyte hydrogels shows interesting results. For the balanced polyampholyte hydrogel charges ranging from 0mM to 160mM we observe a negative slope in the steady state potential whereas we observe a positive slope in the steady state potential for the highest charged balanced polyampholyte hydrogel, which is 200mM in this case. The membrane potential formed due to both Donnan and Diffusion potential could have played a vital role in these changes in the slope from negative to positive. Out of the two potentials one could have dominated earlier which could have given the negative slope and later for the higher charged balanced polyampholyte hydrogel the other potential could have dominated the one, which dominated earlier which leads to a positive slope in the steady state potential. Additionally, we need to consider the case of Streaming potentials, especially in the case

that inequalities in pressure heads or osmotic pressure differences be observed, which could also be the reason in the change of the slope from negative to positive.

CHAPTER 4: DETECTION OF BACTERIAL PROLIFERATION AND MICRO MOTION

ABSTRACT

The ability to monitor bacterial proliferation and micro motion on synthetic hydrogels has a number of important potential applications in biomedicine. In particular, this has important applications in understanding bacterial infections, living biosensor development, and bacterial-biomaterial adhesive interactions. Using image processing algorithms and a well-defined synthesis and characterization of hydrogel surfaces, this study examines the surface charge dependent growth and motion of the bacteria Pseudomonas fluorescens 5RL on synthetic biomaterial surfaces. A series of ionic hydrogels were chosen as substrates for bacterial adhesion and growth and characterized using thermodynamic analysis, diffusion potential measurements, and swelling equilibrium measurements. Trajectory and velocity components were acquired and examined for bacteria populations on different charged hydrogel surfaces. A sequence of images was acquired using a Ziess Axiovert 35 phase contrast microscope with a National Instruments charge coupled device camera and frame grabber. The images were analyzed and processed individually to improve their quality using background removal, filtering, binary image conversion, and edge detection. Cells within a given region of interest were counted and tracked from one frame to the next. A stochastic analysis of the bacterial movement showed surface dependent and population dependent motion correlated with the hydrogel thermodynamic state.

I. INTRODUCTION

The study of synthetic hydrogels is at the boundary between polymer physics and biophysics. Synthetic hydrogels, which are usually biologically inert materials, may be modified with protein fragments to modulate cell behavior at the biomaterial-tissue interface [30-32, 61-63]. From the polymer point of view, Polyampholytes are challenging heteropolymers containing monomers of both positive and negative charges, with properties that are very different from those of conventional Polyelectrolyte polymers, which contain monomers of only one charge sign. The ability to monitor bacterial proliferation and micro motion on synthetic hydrogels has a number of important potential applications in biomedicine. In particular, this has important applications in understanding bacterial infections, living biosensor development, and bacterial-biomaterial adhesive interactions. Bacterial adhesion has traditional been described using the DLVO (Derjaguin, Landau, Verwey, and Overbeek) theory [64] in which the adhesion is modeled using a combination Lifshitz-Van der Waals and electric double layer interactions. Lewis acid-base or hydration interactions are included in the DLVO theory as the XDLVO theory. The supporting matrix consists of a synthetic hydrogel which can be fabricated with varying charge densities. The bacterial cell surface has a net negative charge under most conditions. Charged groups on the bacterial surface or the supporting matrix may change its charge. Using image processing algorithms and a well-defined synthesis and characterization of polyelectrolyte hydrogel surfaces, this study examines the surface charge dependent growth and motion of the bacteria *Pseudomonas fluorescens* 5RL on synthetic biomaterial surfaces. A series of

ionic hydrogels were chosen as substrates for bacterial adhesion and growth and characterized using thermodynamic analysis, diffusion potential measurements, and swelling equilibrium measurements.

This study has been done to determine the bacterial proliferation and micro motion on a Balanced Polyampholyte Hydrogel and an unbalanced Polyelectrolyte Hydrogel. A movie is taken with bacteria attached to the Polyampholyte Hydrogel and unbalanced Polyelectrolyte Hydrogel. The movie is converted into sequence of frames and is taken to analyze and process individually, and then a target containing isolated bacteria is taken in order to find its micro motion in the hydrogel surface. Growth pattern of the bacteria over the hydrogel surface is also noted and the necessary figures obtained during various processing of the images are also shown

.

II. MATERIALS AND DESIGN

A. PREPARATION OF HYDROGELS

Balanced Polyampholyte hydrogels were synthesized by mixing the monomers 2-sulfoethyl methacrylate (SEMA-H) or 2-methacryloxyethyltrimethylammonium chloride (MAETA-Cl) in varying proportions with the neutral monomer 2-hydroxyethyl methacrylate (HEMA) where SEMA and MAETAC are strongly acidic and basic monomers. Specifically, the 2.00 M HEMA solution was mixed with one of the 2.00 M charged monomer stock solutions, to yield a total volume of 10 mL. In this way,

copolymers with charge offsets spaced between 0 and ± 200 mM were made. Similarly for Polyelectrolytes, Copolymer hydrogels were synthesized by mixing the 1.54 M of monomer MAETA-Cl stock solution in varying proportions with the 1.54 M Poly (ethylene glycol) (1000) dimethacrylate (PEGDMA) or 2-hydroxyethyl methacrylate (HEMA) solution to yield a total volume of 10 mL. And the copolymers with logarithmically spaced charge offsets between 0 and ± 1540 mM were made in the same way as Polyampholytes. The monomers SEMA-H and MAETA-Cl were chosen since they are highly dissociated over a wide range of pH and ion strengths. Hydrogel membranes were formed by casting several milliliters of the pregellation solution between two glass plates separated by a thin Teflon film spacer. Small metal binder clips were used to form a tight seal between the two plates. After polymerization was complete, the hydrogels were removed from between the glass plates and placed in distilled deionized water where they were washed continuously with daily water changes for two weeks. In this way, residual non-polymerized chemicals were removed from the gels.

B. BACTERIAL CELL CULTURE

Bacteria was started from a frozen primary stock kept at -70^{o}C. One mL of the frozen stock was placed in 100 mL sterilized LB media containing 100 μL of tetracycline and the mixed solution is placed in the incubator, which provides the environment suitable for the bacteria to grow. After 24 hours the bacteria was restarted by taking 1 mL of the previous bacterial solution and placed in a new flask of 100 mL sterilized LB media

containing 100 μL tetracycline to prepare a new bacterial stock solution. Tetracycline at a concentration of 1 μL/mL of media was used to prevent contamination. After 4-8 hours this new stock solution was used for the experiments. The additional passage in this step is necessary to allow the bacterial to re-adjust after being frozen down. To inoculate the hydrogel samples, 9.8 mL of LB media was mixed with 200 μL of the bacterial solution in a 15 mL centrifuge tube. After the diluted bacterial samples were mixed thoroughly, 2 mL of the solution was added to a hydrogel disk in a 12 well culture plate. This dilution produced a sparse population of bacterial cells upon the initial inoculation.

C. IMAGE PROCESSING METHOD

After the hydrogel membrane is ready, bacteria is inoculated over the hydrogel surface to detect the micro motion of bacteria *Pseudomonas fluorescens* 5RL over the balanced Polyampholyte and unbalanced Polyelectrolyte hydrogels. Trajectory and velocity components were acquired and examined for bacteria populations on different charged hydrogel surfaces. A sequence of movie files in the AVI format for every half an hour for 5 hours were acquired by placing the dish containing the bacteria with the hydrogel surface using a Ziess Axiovert 35 phase contrast microscope with a National Instruments charge coupled device camera and frame grabber and a Lab view program. The AVI files were processed and analyzed using a MATLAB algorithm with Image Processing Toolbox to improve their quality using background removal, filtering, binary image conversion, and edge detection for calculating the Bacterial Density for different

timescale. Cells within a given region of interest were tracked from one frame to the next for detecting the micro motion of the bacteria over these Biomaterials.

1. Pre-Processing Method

A LABVIEW program has been used to capture the video file for 2 minutes for every half an hour for continuous 5 hours and store it as an AVI file using the Ziess Axiovert 35 phase contrast microscope with a National Instruments charge coupled device camera and frame grabber. The AVI files captured is very big in its file size and in order to give these files to the MATLAB for post processing, the AVI files are segmented into small files to reduce its size so that it can be accepted by MATLAB using ADOBE Premiere Pro software. In this way AVI files are captured and segmented for all Polyampholyte charged hydrogels and Polyelectrolyte charged hydrogels.

2. Post-Processing Method

The segmented AVI files obtained are now given to a MATLAB program that can count the growth of the bacteria and also detect the micro motion of the bacteria over the hydrogel surface. The MATLAB algorithm for counting the bacteria and track the bacterial micro motion has been explained clearly below.

i. Processing of Individual frames

The Matlab Program reads the AVI file and converts the entire video file into a sequence of frames and each individual frames are processed separately in order to improve the image quality. First, in order to avoid the dimension mismatch for further processing, each frame which is a color map image is converted into a gray scale image by eliminating the hue and saturation information while retaining the luminance. Tophat and bottom-hat filtering can be used together to enhance contrast and to correct uneven illumination in an image when the background is dark. The procedure is to add the original image to the tophat-filtered image, and then subtract the bottom-hat-filtered image to get the enhanced image. The original image is converted into a binary image and filters like Median filters are used to reduce the noises and other small particles other than bacteria in the binary image whose intensity value lies in the range [0 to 1]. A proper edge detection method is applied to find the edge of the bacteria and once the edges are fixed, the image is subjected to dilation, morphological opening and closing to fill the gaps between the circles and by smoothening their outer edges in order to provide the original shape and size for the bacteria and removing smaller particle other than the bacteria. In this way the remaining frames are subjected to these processing techniques to improve the image quality and also to carefully count the bacteria attached to the hydrogel surface.

ii. Detecting the Micro motion of the Bacteria

To detect the micro motion of the bacteria, the AVI files of the first 30 mins video containing the bacterial micro motion over the balanced Polyampholytes and unbalanced polyelectrolytes is taken for the analysis. The AVI files are treated in the same way as counting techniques by processing each frame using various methods. Once the processed frames are obtained, a cropping region is used to isolate single bacteria from the entire frame and similarly the same cropping region is applied for the remaining frames of the AVI file such that the same singe bacteria can be located within that cropped region for the entire AVI file. Similarly another cropping region can be used to locate any other different bacteria. The cropped region containing the bacteria can be displayed as a movie to show the single bacterial micro motion over the hydrogel surface. Using 'bwlabel' and 'regionprops' in Matlab, the centroid of the same bacteria in the all the frames of the entire AVI file can be found. If there is any focal length problem or the bacteria moves deeper into the hydrogel surface, the targeted bacteria may not be visible in the entire cropped frame, so care must be taken to check each cropped region. The algorithm is built in a way such that if there are no bacteria in the cropped region then neglect the current frame and go for the next frame. The centroid gives the position of the bacteria over the hydrogel surface in terms of numerical values. Thus by finding the centroid of the bacteria, the bacterial micro motion over balanced Polyampholytes and unbalanced Polyelectrolytes can be found.

III. RESULTS AND DISCUSSION

Bacterial adhesion is a complicated process that is affected by many factors including the bacteria (hydrophobicity, surface charge etc.), the material surface (chemical composition, roughness, configuration, wettability) and environmental factors (temperature, bacterial concentration etc,). Using Image processing techniques, this study shows that the chemical composition of balanced polyampholyte and unbalanced polyelectrolyte hydrogels influences the bacterial adhesion and growth rates. Polyethylene glycol hydrogels are more resistant to bacterial adhesion than HEMA materials. **Figure A3-23** shows the clear image of the bacteria *Pseudomonas fluorescens 5RL* taken from a transmission electron microscopy and the sample microscopic image in the **Figure A3-24,** shows the bacteria attaching over the hydrogel surface. The **Figure A3-25** is taken from the AVI file and this image is subjected to image processing techniques like Top-hat and Bottom-hat filtering (**Figure A3-26),** edge detection (**Figure A3-27),** dilation (**Figure A3-28),** median filtering (**Figure A3-29),** morphological closing (**Figure A3-30)** and morphological opening (**Figure A3-31).** The final image in the **Figure A3-32** shows clearly the bacteria in the white spot**. Figure A3-33** shows the bacteria in different colors in order to identify the individual bacteria from the neighboring bacteria. In **Figure A3-34**, the bacterial growth curves for a neutral polyampholyte and balanced polyampholytes have been plotted using the data obtained by counting the white spot using image processing techniques as mentioned earlier in the method section. The **Figure A3-34**, the bacterial growth on polyampholytic hydrogels show that the pure HEMA hydrogel produce a large increase in the growth rate compared

to polyampholyte hydrogels with a balanced concentration of positive and negative charge densities, whereas the growth curves of the charged balanced polyampholytic hydrogels show to be accumulating at the same region. **Figure A3-35** shows the 3-D plot of the bacterial micro motion over pure HEMA hydrogel surface with respect to time. The bacterial micro motion on balanced polyampholytes as shown in the **Figure A3-36**, doesn't show any systematic pattern, whereas, **Figure A3-37** showing the micro motion of the bacteria on unbalanced polyelectrolyte hydrogels shows a systematic decrease in micro motion with increasing positive charge offset. These results are consistent with the influence of both hydrophobic and electrostatic forces on the growth and the motion of the bacteria *Pseudomonas fluorescens 5RL.*

IV. CONCLUSION

Compare to neutral HEMA hydrogels, copolymer HEMA hydrogels with balanced charge densities in the range of 40 mM to 160 mM show decreased proliferation rates of the bacteria *Pseudomonas fluorescens 5RL*. The increase in the growth rate for the neutral HEMA hydrogels could be due to the point that the HEMA gels are more attractive and active as the osmotic pressure is high in these neutral hydrogels and it could be also due to the free positive ions available in these neutral hydrogels formed during the polymerization reaction. The bacterial micro motion over balanced polyampholyte hydrogels to increasing concentration of balanced charges does not show a systematic change in its micro motion. Unlike polyampholyte hydrogels, increasing charges for

polyelectrolyte hydrogels produces considerable decreased bacterial motion as the bacteria carrying the negative charge get attached to the available positive charges on the strong basic polyelectrolyte hydrogels and hence their motion over the gel surfaces are restricted when the polyelectrolyte charges are increased.

CHAPTER 5: CONCLUSIONS

I. INTRODUCTION

The purpose of this master's thesis was to present a definitive study about the balanced polyampholyte hydrogels, the diffusion potential measurement and the bacteria-hydrogel interactions which could perhaps helps to make improvements to its application in variety of fields. Chapters were organized to explain and understand the principles and the concepts behind each experiment dealing with the balanced polyampholyte hydrogels. The introduction chapter served as a general study explaining about the hydrogels, its chemical and physical properties and also about the development of first soft contact lenses by Wichterle in 1961. The importance of hydrogel in medical field due to its biocompatibility and the general application of hydrogels in various fields have been discussed more clearly. The significance of balanced polyampholyte hydrogels both in chemical as well as in physical properties was discussed and also the needs to understand about its characteristic to widen its applications are stated. Swelling behavior and the phase transition of balanced polyampholytic hydrogels were taken for the second chapter and the theory section is included to explain about the free energy model of the balanced polyampholyte hydrogel. The swelling measurement results are examined with the theoretical understanding of the properties of polyampholyte hydrogel. The membrane potential measurement and the theory involved in it were studied in the third chapter and a series of balanced polyampholyte hydrogel were subjected to the membrane potential measurement and the results are analyzed. The application of digital image processing techniques to understand the interactions of Pseudomonas fluorescens 5RL on the balanced polyampholyte hydrogel were focused in the chapter 4 and these interaction

results are compared with the unbalanced polyelectrolyte hydrogel (strong basic hydrogels). In summation, the population density and the micro motion of the bacteria over the hydrogel surfaces are found using a proper image processing technique.

II. PART CONCLUSIONS

Chapter 2 has discussed the preparation of a series of balanced Polyampholyte hydrogels and their corresponding thermodynamic behaviors. The phase transition of Polyampholyte hydrogels has been shown and necessary theoretical background has been provided. The swelling response of polyampholyte hydrogels near the balance point in DI water, 1.54mM Nacl, PBS and 1.5M Nacl is obtained and the **Table 2.1**, **Table 2.2**, **Table 2.3** shows the respected data obtained for the swelling response of the hydrogels for the above bath solutions and for different time periods. As seen from the graph plotted in the **Figure A3-3** with the initial swelling measurement of the hydrogels taken on Jan 30th of different charge concentration after washed with DI water, it has been shown that there is a slight swelling transition in the hydrogels due to the fact that the ion chemical potentials in the bath and hydrogel phases must be equal in equilibrium even for DI water having no added salt in it, as even when the pH is 7 the electrostatic inclusion of hydrogen or hydroxide ions can create very low or high internal pH values, depending on the polymer charge density and it could cause the swelling pattern in the hydrogels. When the hydrogels washed with 1.54mM Nacl solution, there is a deswelling pattern as shown in the **Figure A3-7**and **Figure A3-9** for all the hydrogels which shows the

polyelectrolyte screening taking effect in this cases as the bath salt concentration increases, the osmotic pressure difference between the hydrogel and the surrounding bath decreases, which results in a deswelling pattern. **Figure A3-11** provides the graph for the swelling measurement of the hydrogels for the 1 x PBS bath solution and the graph doesn't show any difference in swelling pattern. When the hydrogels are allowed to wash in DI water again, we see a swelling pattern in the hydrogels as shown in the graph plotted in **Figure A3-13** due to the increase in the cations in the hydrogel phase, which increases the osmotic pressure. The hydrogels are again washed with higher salt concentration i.e. 1.5M Nacl salt concentration. Balanced Polyampholyte hydrogels are expected to swell at higher salt concentration due to the ionic dissociation, but **Figure A3-15** shows a deswelling pattern, which founds to be abnormal. These results show that polyampholyte hydrogels exhibits properties similar to polyelectrolyte hydrogels and collapse at intermediate bath ionic salt concentration. But instead of swelling in the higher salt concentration our result shows that there is a deswelling pattern. This study has given an importance in the selection of the monomers used in the preparation of these hydrogels, the micro structural arrangement of the monomeric groups during polymerization reaction and to the counterions in the hydrogel phase of the balanced Polyampholyte hydrogels, which could turn the actual property of these hydrogels. The deswelling of the balanced Polyampholytic hydrogels inspite of swelling during the inclusion of high salt concentration could be due to the mentioned reason and also due to the micro structural arrangement of charged and neutral monomers during the polymerization reaction which could have played a role in the decrease of the osmotic pressure difference between the hydrogel phase and the bath phase.

In chapter 3, the membrane potential measurements were studied and examined for a series of balanced polyampholyte hydrogel. In **Figure A3-16, Figure A3-17, Figure A3-18, Figure A3-19, Figure A3-20,** the measured voltage for the hydrogel with charges 0mM, 40mM, 80mM, 120mM and 160mM respectively, is found to be following the same pattern as the membrane potential goes through a minimum as the electrolyte concentration increases, and following a negative slope with the increase in the Nacl salt concentration. When we examine the result of 200mM Polyampholyte hydrogel as shown in the graph plotted in the **Figure A3-21**, the membrane potential goes through a maximum as the electrolyte concentration increases and follows a positive slope. The reason for this change in the slope from negative to positive could be due to the membrane charge density, which is higher when compared to the remaining charged hydrogels. The membrane potential formed due to both Donnan and Diffusion potential could have played a vital role in these changes in the slope from negative to positive. Out of the two potentials one could have dominated earlier which could have given the negative slope and later for the higher charged balanced polyampholyte hydrogel the other potential could have dominated the one, which dominated earlier which leads to a positive slope in the steady state potential. Additionally, we need to consider the case of Streaming potentials, especially in the case that inequalities in pressure heads or osmotic pressure differences be observed, which could also be the reason in the change of the slope from negative to positive. We can also note from the results that the initial voltage obtained for all the hydrogel charges during the measurement is found to be decreasing with increase in the hydrogel charges. This may be due to the reduced flow of charges in

the Nacl solution from one chamber to another with increase in the membrane charge in between the two chambers.

Chapter 4 explains the application of image processing techniques to examine the bacteria *Pseudomonas fluorescens 5RL* and the hydrogel interactions. Image processing techniques are applied and the resulting images are shown. The final image in the **Figure A3-32** after various processing techniques clearly shows the bacteria in the white spot**.** **Figure A3-33** shows the bacteria in different colors in order to identify the individual bacteria from the neighboring bacteria. In **Figure A3-34**, the bacterial growth curves for a neutral polyampholyte and balanced polyampholytes have been plotted using the data obtained by counting the white spot using image processing techniques as mentioned earlier in the method section. Compare to neutral HEMA hydrogels, copolymer HEMA hydrogels with balanced concentration of positive and negative charge densities in the range of 40 mM to 160 mM show decreased proliferation rates of the bacteria *Pseudomonas fluorescens 5RL* as shown in the graph plotted in the **Figure A3-34**. The increase in the growth rate for the neutral HEMA hydrogels could be due to the point that the HEMA gels are more attractive and active as the osmotic pressure is high in these neutral hydrogels and it could be also due to the free positive ions available in these neutral hydrogels formed during the polymerization reaction. **Figure A3-35** shows the 3-D plot of the bacterial micro motion over pure HEMA hydrogel surface with respect to time. The bacterial micro motion over balanced polyampholyte hydrogels to increasing concentration of balanced charges as shown in the **Figure A3-36** does not show any systematic pattern in its micro motion. Unlike polyampholyte hydrogels, increasing charges for polyelectrolyte hydrogels produces considerable decreased bacterial motion

as the bacteria carrying the negative charge get attached to the available positive charges on the strong basic polyelectrolyte hydrogels and hence their motion over the hydrogel surfaces are restricted when the polyelectrolyte charges are increased and it is shown clearly in the **Figure A3-37**. These results are consistent with the influence of both hydrophobic and electrostatic forces on the growth and the motion of the bacteria *Pseudomonas fluorescens 5RL.* Using Image processing techniques, this study shows that the chemical composition of balanced polyampholyte and unbalanced polyelectrolyte hydrogels influences the bacterial adhesion and growth rates

II. THESIS CONCLUSION

The purpose of this Masters thesis was to present a definitive study about the balanced polyampholyte hydrogels in particular. The influence of the physical and the chemical properties of the hydrogels are well understood and analyzed with the swelling behavior of the hydrogels for different bath solutions, diffusion potential measurement of the hydrogel and finally the bacteria to hydrogel interactions. Swelling transition seems to follow at low ionic salt concentration as the ion chemical potentials in the bath and hydrogel phases must be equal in equilibrium even for DI water having no added salt in it, as even when the pH is 7 the electrostatic inclusion of hydrogen or hydroxide ions can create very low or high internal pH values, depending on the polymer charge density and it could cause the swelling pattern in the hydrogels and a deswelling at the intermediate ionic salt concentration showing the polyelectrolyte effects due to the loss in the charge

densities and the osmotic pressure difference between the hydrogel and the surrounding bath decreases. We see a deswelling pattern instead of swelling in the hydrogel even when the ionic salt concentration is increased further. This could be due to the counterion effects and the micro structural arrangements of the monomer that could have decreased the osmotic pressure difference between the hydrogel phase and the bath phase. When the diffusion potential measurement is concerned, for the balanced polyampholyte hydrogel charges ranging from 0mM to 160mM we observe a negative slope in the steady state potential whereas we observe a positive slope in the steady state potential for the highest charged balanced polyampholyte hydrogel, which is 200mM in this case. The membrane potential formed due to both Donnan and Diffusion potential could have played a vital role in these changes in the slope from negative to positive. Additionally, we need to consider the case of Streaming potentials, especially in the case that inequalities in pressure heads or osmotic pressure differences be observed, which could also be the reason in the change of the slope from negative to positive. The bacteria

Pseudomonas fluorescens 5RL and the balanced polyampholyte hydrogel interactions are examined using proper image processing techniques and the results are compared with the bacteria and unbalanced polyelectrolyte hydrogels interactions. For polyampholytes compare to neutral HEMA hydrogels, copolymer HEMA hydrogels with balanced charge densities in the range of 40 mM to 160 mM show decreased proliferation rates of the bacteria *Pseudomonas fluorescens 5RL*. The bacterial micro motion over balanced polyampholyte hydrogels to increasing concentration of balanced charges does not show a systematic change in its micro motion. Unlike polyampholyte hydrogels, increasing charges for polyelectrolyte hydrogels produces considerable decreased bacterial motion

as the bacteria carrying the negative charge get attached to the available positive charges on the strong basic polyelectrolyte hydrogels and hence their motion over the gel surfaces are restricted when the polyelectrolyte charges are increased. Overall of this thesis makes the importance in the selection of the acidic and basic monomers used in the preparation of these hydrogels, the micro structural arrangement of the monomeric groups during polymerization reaction and to the counterions in the hydrogel phase of the balanced polyampholyte hydrogels which all could influence in the turn of the actual property of balanced polyampholyte hydrogels.

A. FUTURE WORK

After understanding the swelling behavior of neutral and balanced polyampholyte hydrogels, we can extend our research to analyze the swelling characteristics of positive and negative hydrogels which may be useful in the applications of controlled drug delivery technology, one of the areas hydrogels have played a key role. Since hydrogels are obtained from hydrophilic polymers with covalent bonding between macromolecules, resulting in a network that is able to absorb large amounts of water, hydrogels allow the normal flow of body fluids responsible for cell maintenance. Since they are physically similar to soft tissues, especially articular cartilage, hydrogels can be designed to have appropriate mechanical properties and may be used as a graft for the repair of articular cartilage defects. Their surface and functional properties should provide the necessary mechanical support for the joint. In order to study the swelling behavior of the hydrogels,

it is necessary to confirm the purity of the chemicals used for the hydrogel preparation in order to avoid the effects caused by the contamination as we have noted in the results of this thesis.

The interactions of bacteria with the hydrogels reveals that surface chemistry influence the bacterial adhesion. However, the relative importance of these factors has not been clearly understood yet. Refinement of the techniques for measuring bacteria-material interactions with reference materials would improve our knowledge of this important, yet complex phenomenon. Understanding the interactions of bacteria with the hydrogels can be used to prevent the bacteria to adhering to the hydrogel implants and/or clean the implants fouled with the bacterial infections and also can be used in the development of biosensors as the bacteria *Pseudomonas fluorescens 5RL* is capable of producing bioluminescence.

REFERENCES

1. Junji Watanabe, Y.K., Kwang Woo Nam, Kazuhiko Ishihara, *Encyclopedia of Biomaterials and Biomedical Engineering.*

2. Wheeler JC, W.J., Cox MJ, Cantrell RW, Watkins FH, Edlich RF, *Evolution of hydrogel polymers as contact lenses, surface coatings, dressings, and drug delivery systems. J Long Term Eff Med Implants*, 1996. **6(3-4):207-17**.

3. D.D. Rossi, *Trans.Am.Soc.Artif.Inter.Orgtans*, 1986. **XXXII:157**.

4. A.S.Hoffman, *J.Controlled Release*, 1987. **6:297**.

5. A.S.Hoffman and .B.D. Ratner, *Synthetic Hydrogels for Biomedical Applciations.* ACS Symposium Series, 1976. **31,p.1**.

6. A.S.Hoffman, A.Afrasiabi, and L.C.Dong, *J.Controlled Release*, 1986. **4:213**.

7. Y.Osada, K.Umezawa, and A.Yamauchi, *Makromol. Chem*, 1988. **189:597**.

8. Seigel, R.A., *Implantable, Self-Regulating Mechanochemical Insulin Pump.* The Regents of the university of California, 1991.

9. M.Suzuki and Y.Sawada, *J.Appl.Phys*. 51:5667 (1980)

10. M.Suzuki, T.Tateishi, T.Ushida, and S.Fujishige, *Biorheol*, 1986. **23:274**.

11. P.Verdugo, *J.Biophys*, 1986. **49:231a**.

12. P.Verdugo, *Rev.Physiol*, 1990. **52:157**.

13. Kantor.Y, K.M., Li.H, *Phys.Rev.E*, 1994. **1383-1392**.

14. Kantor.Y, K.M., *Phys.Rev.E*, 1995. **835-846**.

15. Carmen Alvarez-Lorenzo, H.H., Kazunori Tanaka, Kimani Stancil, Alexander YU. Grosberg, and Toyoichi Tanaka, *Simultaneous Multiple_point Adsorption Of Aluminium Ions And Charged Molecules by a Polyampholyte Thermosensitive Gel: Controlling Frrustrations in a heteropolymer Gel. Langmuir*, 2001. **17**.

16. Gutin.A.M, S.E.I., *J.chem.Phys*, 1994. **R3322**.

17. Kantor.Y, Kardar.M., *Phys.Rev.E*, 1995. **51**,**1299**.

18. Kantor.Y, Kardar.M., *Phys.Rev.E*, 1995. **52**,**835**.

19. Wittmer.J, J.A., Joanny.J.F, *Europhys.Lett*, 1993. **24**(263).

20. Victor.J.M, I.J.B., *Europhys.Lett*, 1993. **24**(189).

21. Anthony E.English, Salvador.Mafe, Jose A.Manzanares, Xiahong Yu, Alexander Yu.Grosberg, Toyoichi Tanaka, *Equlibrium swelling properties of polyampholytic hydrogels. J.chem.Phys*, 1996. **104(21)**.

22. G.Nisato, J. P.Munch and S. J.Candau, *Swelling,Structure, and Elasticity of Polyampholyte Hydrogels. Langmuir*, 1999. **15**.

23. Baker.J.P, Stephens.D.R., Blanch.H.W, Prausnitz.J.M, *Macromolecules*, 1992. **25**(1955).

24. Annaka.M, Tanaka.T. *Nature*, 1992. **355**(430).

25. Baker.J.P, Blanch.H.W., Praustnitz.J.M, *Polymer*, 1995. **36**(1061).

26. Katayama.S, Myoga.A., Akahori.Y, *J.Phys.Chem*, 1996. **96**(4698).

27. Kudaibergenov.S.E, *Ber.Bunsen-Ges. Phys.Chem*, 1996. **100**(1079).

28. Than.L.T.M, Makhaeva.E.E., Khokhlov.A.R, *Polym.Gels Networks.* 1997. **5**(357).

29. Mafe.S, Manzanares.J.A., English.A.E,Tanaka.T, *Phys.Rev.Lett*, 1997. **79**(3086).

30. Hern.DL, Hubbell.J.A., *Incorporation of adhesion peptides into nonadhesive hydrogels useful for tissue resurfacing. J.Biomed Mater Res*, 1998. **39**(266-76).

31. Shin H, Jo.s., Mikos A.G, *Modulation of marrow stromal osteoblast adhesion on biomimetric oligo[poly(ethylene glycol)fumarate] hydrogels modified with arg-gly asp peptides and a poly(ethyleneglycol) spacer.* J.*Biomed Mater Res*, 2002. **61**(169-79).

32. Gobin A.S, West.J.L., *Cell Migration through defined synthetic ECM analogs.* Faseb J, 2002. **16**(751-3).

33. Elbert DL, Hubbell JA. Conjugate addition reactions combined with free radical cross-linking for the design of materials for tissue engineering. *Biomacromolecules* 2001,**2;430-41**

34. Esfandiar Behravesh, vassilios I, Sikavitsas, Antonios G.Mikos. Quantification of ligand surface concentration of bulk-modified biomimetic hydrogels. *Biomaterials*, 2003.**4365-4374**

35. Shahinpoor, *Microelectromechanics of ionic polymer gels as electrically controllable artificial muscles.* Journal of Intelligent Meterial Systems and Structures, 1995. **307-314**.

36. Osada, Y.and S.B.R., *Intelligent Gels.* Scientific American, 1993. **268(5)**: p. pp.82-87.

37. F. Helfferich, *Ion Exchange.* 1962.

38. Lakshminarayanaiah, N., *Transport Phenomena in Membranes.* 1969.

39. Oss, C. J. v. (1991) *Biofouling* **4**, 25-35 .

40. Klotz, S. A. (1990) in *Microbial Cell Surface Hydrophobicity*, eds. Doyle, R. J. & Rosenberg, M. (Am. Soc. Microbiol., Washington, DC), pp. 107-136.

41. Loosdrecht, M. C. M. v., Lyklema, J., Norde, W., Schraa, G. & Zehnder, A. J. B. (1987) *Appl. Environ. Microbiol.* **53**, 1898-1901 [ISI][Medline].

42. Mozes, N., Marchal, F., Hermesse, M. P., Haecht, J. L. V., Reuliaux, L., Leonard, A. J. & Rouxhet, P. G. (1987) *Biotechnol. Bioeng.* **30**, 439-450 [ISI].

43. Busscher, H. J., Weerkamp, A. H., Mei, H. C. v. d., Pelt, A. W. J. v., Jong, H. P. D. & Arends, J. (1984) *Appl. Environ. Microbiol.* **48**, 980-983 [ISI][Medline] .

44. Ofek, I. & Doyle, R. J. (1994) *Bacterial Adhesion to Cells and Tissues* (Chapman & Hall, New York).

45. Fletcher, M. & Pringle, J. H. (1985) *J. Colloid Interface Sci.* **140**, 5-13.

47. X.Yu, Ph.d. thesis, Massachusetts Institute of Technology, 1993.

48. A.English, X.Yu and T. Tanaka, Abstract. Materials Research Society, N3.58, 1995.

49. Sarkyt E. Kudaibergenov*, a.V.B.S., *Swelling, Shrinking, Deformation, and Oscillation of Polyampholyte Gels Based on Vinyl 2-Aminoethyl Ether and Sodium Acrylate†.* Langmuir, 1999. **Vol. 15**(No. 12).

50. A.E.English, Toyoichi.T., Elazer R.Edelman, *Polyampholytic Hydrogel Swelling Transitions: Limitations of the Debye-Huckel Law.* Macromolecules, 1998. **31**.

51. Anthony E.English, Elazer.R.Edelman, Toyoichi Tanaka, *Polymer Hydrogel Phase Transitions.* Macromolecules, 2000.

52. A.J. Grodzinsky and P.E. Grimshaw,"Electrically and chemically controlled hydrogels for drug delivery,"*Pulsed ans self-Regulated Drug Delivery*, pp. **47-64**, 1990

53. N.A.Peppas and L. Brannon-Peppas,"Solute and penetrant diffusion in swellable polymers.IX. The mechanism of drug release from pH-sensitive swelling-controlled systems," *J.Control.Release*,pp.**267-274**

54. A.V.Dobrynin, M.Rubinstein. *J.Phys.II* 1995, **5, 677**

55. P.G.Higgs, J.Joanny. *J.Chem.Phys*. 1991, **94, 1543**

56. Y.Chu, P.P.V., M.J.McGlade ans S.Varanasi, *pH-induced swelling kinetics of polyelectrolyte hydrogels.* J.Appl.Polymer Sci, 1995. **58**.

57. A. Szymczyk, P.F., J.C. Reggiani, J. Pagetti, *Characterisation of surface properties of ceramic membranes by streaming and membrane potentials.* J.Membrane Sci, 1998. **146**(277-284).

58. R.Schlogl, *Electrolyte seperation of ions by ion-exchange membranes.* Phys.Chem, 1978. **82**(225).

59. Tzu-Jen Chou, A.T., *Ionic behavior across charged membranes in methanol±water solutions. I: Membrane potential.* J.Membrane Sci, 1998. **144**(275-284).

60. N. Lakshminarayanaiah, Equations of Membrane Biophysica, Academic Press, Orlando, 1984.

61. Drumheller P.D, E.D.L., Hubbell.J.A, *Multifunctional poly(ethylene glycol) semi-interpenetrating polymer networks as highly selective adhesive substrates for bioadhesive peptide grafting.* Biotechnol Bioeng, 1994. **43**(772-80).

62. Healy K.E, R.A., Stile.R.A, *Designing biomaterials to direct biological responses.* Ann N Y Acad Sci, 1999. **875**(24-35).

63. Rezannia.A, H.K.E., *Biomimetic peptides surfaces that regulate adhesion,spreading,cytoskeletal organization,a nd mineralization of the matrix deposited by osteoblast-like cells.* Biotechnol Prog, 1999. **15**(19-32).

64. Morra.M, C.C., J.Biomater.Sci, 1997. **9(1)**(55-74).

APPENDIX 1: TABLES

A1-1: HEMA Stock solutions

100 mL 2 M HEMA Stock
25.686 mL HEMA
40 mL EG
387 µL EGDMA
1 mL 4 wt% APS
Fill to 100 mL with H2O

A1-2: SEMA-MEATAC Stock solutions

12mL 1 M SEMA-MEATAC Stock
7.792 mL SEMA-MEATAC
4.8 mL EG
46.44 µL EGDMA
120 µL 4 wt% APS
Fill to 12 mL with H2O

A1-3: PEGDMA Stock solutions

450 mL 1.54M PEGDMA Stock
90.187 mL PEGDMA
180 mL EG
1749 µL EGDMA
0.4g/10mL 4 wt% APS
Fill to 450 mL with H2O

A1-4: MAETAC Stock solutions

50 mL MAETAC Stock
20.770 mL MAETAC
20 mL EG
194 µL EGDMA
100 µL 4 wt% APS
8.536 mL H2O

TableA1-5: Polyampholyte Hydrogel Recipe

Chemical Property	Chemical	F.W / d / %	Conc.	Mass / Volume
Neutral Monomer	HEMA(2-hydroxyethyl methacrylate)	130.14 / 1.034 / 98%	2.0 M	25.686 mL / 100 mL
Acidic Monomer (-)	SEMA(2-sulfoethyl methacrylate)	196.1/1.2 / 95%	2.0 M	8.600 mL / 25 mL
Basic Monomer (+)	MAETAC(Methacryloethyl trimethyl ammonium chloride)	207.7 / 70%	2.0 M	2.9672 mL / 10 mL
Solvent	EG(Ethylene Glycol)			40 mL / 100 mL or 4 mL / 10mL
Cross-linker	EGDMA(ethylenglycol dimethacrylate)	198.22/1.057/98 %	20.2 mM	387 uL / 100 mL or 39 uL/ 10 mL
Free Radical Initiator	APS(ammonium persulfate)	228.2	1.76 mM	1 mL 4 wt% / 100 mL or 100 uL / 10 mL
Initiator	SMBS(sodium metabisulphite)	190.1	7.6 mM	100 uL 15 wt% / 10 mL

TableA1-6: Polyelectrolyte Hydrogel Recipe

Chemical Property	Chemical	F.W / d / %	Conc.	Mass / Volume
Monomer	PEGDMA(Poly (ethylene glycol) (1000) dimethacrylate)	1154 / 1.10/20.45%	1.54M	90.187 g / 450 mL
Basic Monomer (+)	MAETAC(Methacryla toethyl trimethyl ammonium chloride)	207.7 / 70%	1.54 M	11.424 mL / 25 mL
Solvent	EG(Ethylene Glycol)			40 mL / 100 mL or 4 mL / 10mL
Cross-linker	EGDMA(ethylenglyco l dimethacrylate)	198.22/1.057/98 %	20.2 mM	387 uL / 100 mL or 39 uL/ 10 mL
Free Radical Initiator	APS(ammonium persulfate)	228.2	1.76 mM	1 mL 4 wt% / 100 mL or 100 uL / 10 mL
Initiator	SMBS(sodium metabisulphite)	190.1	7.6 mM	100 uL 15 wt% / 10 mL

TableA1-7: Membrane Samples

Sample	PA Offset (mM)	HEMA Concentration (mM)	Balanced PA Concentration (mM)	2.0 M HEMA (mL)	2.0 M SEMA+MEATAC (mL)
0	0	2000	0	10.000	0.000
1	40	1960	40	9.800	0.200
2	80	1920	80	9.600	0.400
3	120	1880	120	9.400	0.600
4	160	1840	160	9.200	0.800
5	200	1800	200	9.000	1.000
			Total Volume	**57.000**	**3.000**

TableA1-8: Membrane Samples for Polyelectrolyte Hydrogels

Sample	Log10 Charge	Charge (mM)	PEG (mL)	2.0 M SEMA+MEATAC (mL)
0		0	10.000	0.000
1	0.437520721	2.74	9.982	0.018
2	0.937520721	8.66	9.944	0.056
3	1.437520721	27.39	9.822	0.178
4	1.937520721	86.60	9.438	0.562
5	2.437520721	273.86	8.222	1.778
6	2.937520721	866.01	4.377	5.623
		Total Volume	**61.785**	**8.215**

TableA1-9: Instructions on Preparing 10 X PBS with Ca++ and Mg++

Stuff to Add	To make 4 liters of 10X	To make 2 liters of 10X	To make 1 liters of 10X
$NaH_2PO_4.H_2O$ (monobasic)	10.25 g	5.126 g	2.563 g
$Na_2HPO_4.H_2O$ (dibasic) or Na_2HPO_4 (dibasic, anhydrous)	47.9 g or 42.512 g	23.95 g or 21.256 g	11.975 g or 10.628 g
NaCl	350.64 g	175.32 g	87.66 g
0.1 M $CaCl_2$ or 1.0 M $CaCl_2$	4 mL or 400 µL	2 mL or 200 µL	1 mL or 100 µL
0.1 M $MgCl_2$ or 1.0 M $MgCl_2$	40 mL or 4 mL	20 mL or 2 mL	10 mL or 1 mL

APPENDIX 2: DERIVATIONS AND MATLAB PROGRAM

INTERNAL VOLUME CONSTRAINT AND SWELLING EQUILIBRIUM

Having defined the total volume, temperature (or equivalent solvent quality), and particle numbers as constants, the total Helmholtz Free Energy is an extremum in equilibrium. Swelling equilibrium follows from the internal constraint that the hydrogel and bath phase volume must sum to the total volume, i.e.

$$dF^T = \left(\frac{\partial \Delta F^T}{\partial V^H}\right)_{\chi(T),\{N_i\}} dV^H + \left(\frac{\partial \Delta F^T}{\partial V^B}\right)_{\chi(T),\{N_i\}} dV^B \tag{1.9}$$

and

$$dF^T = \sum_{i=1}^{\sigma}\left[\left(\frac{\partial \Delta F^H}{\partial V}\right) - \left(\frac{\partial \Delta F^B}{\partial V}\right)\right] dV = 0\,, \tag{1.10}$$

where the constraint, $V = V^H + V^B$ and $dV^H = -dV^B$, has been used. In this case volume partials give the osmotic pressures,

$$\Pi_i = -\left(\frac{\partial \Delta F^T}{\partial V}\right)_{\chi(T),\{N_i\}}\,. \tag{1.11}$$

The internal volume constraint therefore leads to osmotic pressure equilibrium [51]

$$-\frac{1}{v}\left[\ln(1-nv) + nv + \chi n^2 v^2\right] + \Pi_{el} + \sum_{i=0}^{\sigma} c_i^H - \sum_{i=0}^{\sigma} c_i^B = 0\,, \tag{1.12}$$

where c^H_i and c^B_i represent the i^{th} ion concentration in the hydrogel and bath phases, respectively. Using the Gaussian elastic free energy approximation gives us an elastic osmotic pressure component,

$$\Pi_{el} = -\frac{\partial \Delta F_{Gel}}{\partial V} = -\frac{n_0}{N_x}\left(\frac{n}{n_0}\right)^{1/3}, \tag{1.13}$$

and by including the Flory modification, the osmotic pressure becomes [51]

$$\Pi_{el} = -\frac{\partial \Delta F_{Fel}}{\partial V} = \frac{n_0}{N_x}\left[\frac{1}{2}\left(\frac{n}{n_0}\right) - \left(\frac{n}{n_0}\right)^{1/3}\right]. \tag{1.14}$$

A closed form solution for the inverse Langevin osmotic pressure is not obvious and so we evaluate this numerically by finding the volume partial derivative of the corresponding free energy.

IONIC DISSOCIATION EQUILIBRIUM

The set of particle numbers in the hydrogel phase are:

$\{N_i\} = \{NA_-, N_{AH}, N_{B+}, N_{BOH}, N_{H+}, N_{OH-}, N_{Na+}, N_{Cl-}\}$

and corresponding set of concentrations

$\{C_i\} = \{CA_-, C_{AH}, C_{B+}, C_{BOH}, C_{H+}, C_{OH-}, C_{Na+}, C_{Cl-}\}$

The set of particles in the bath phase are:

$\{N_{ibath}\} = \{N_{\text{H+bath}}, N_{\text{OH-bath}}, N_{\text{Na+bath}}, N_{\text{Cl-bath}}\}$

$\{C_{ibath}\} = \{C_{\text{H+bath}}, C_{\text{OH-bath}}, C_{\text{Na+bath}}, C_{\text{Cl-bath}}\}$

Electro neutrality in the bath can be written as

$$C_{H^+bath} + C_{Na^+bath} - C_{Cl^-bath} - C_{OH^-bath} = 0$$

Or

$$C_{H^+bath} + C_{Na^+bath} - C_{Cl^-bath} - \frac{K_w}{C_{H^+bath}} = 0$$

Charge electro neutrality for the acidic hydrogel phase

$$C_{H^+} - C_{B^+} - C_{A^-} + C_{Na^+} - C_{Cl^-} - C_{OH^-} = 0$$

Acid and base dissociation equilibrium is equivalent to

$$K_a = \frac{C_{A^-}C_{H^+}}{C_{AH}} \text{ and } \qquad K_b = \frac{C_B C_{H^+}}{C_{B^+}}$$

where K_a and K_b are the acid and base dissociation constants, respectively.

The total concentration of acidic and basic monomers are written as

$$C_{Ao} = C_{AH} + C_{A^-} \qquad \text{and} \qquad C_{Bo} = C_B + C_{B^+}$$

Writing the dissociated acidic monomer concentration using the dissociation equilibrium equation and the definition of the total acidic monomer concentration gives

$$C_{A^-} = \frac{C_{Ao}K_a}{\left(C_{H^+} + K_a\right)} \qquad C_{B^+} = \frac{C_{Bo}C_{H^+}}{\left(C_{H^+} + K_b\right)}$$

Using the Donnan relations we can write the internal chloride and hydroxide ion concentrations in terms of the know bath concentrations

$$\frac{C_{Na^+}}{C_{Na^+bath}} = \frac{C_{H^+}}{C_{H^+bath}} \qquad \text{or} \qquad C_{Na^+} = C_{Na^+bath}\frac{C_{H^+}}{C_{H^+bath}}$$

Similarly,

$$\frac{C_{Cl^-}}{C_{Cl^-bath}} = \frac{C_{H^+bath}}{C_{H^+}} \qquad \text{or} \qquad C_{Cl^-} = C_{Cl^-bath}\frac{C_{H^+bath}}{C_{H^+}}$$

and

$$\frac{C_{OH^-}}{C_{OH^-bath}} = \frac{C_{H^+bath}}{C_{H^+}} \qquad \text{or} \qquad C_{OH^-} = \frac{K_w}{C_{H^+}}$$

Combining the above relations gives

$$C_{H^+} + C_{B^+} - C_{A^-} + C_{Na^+} - C_{Cl^-} - C_{OH^-} = 0$$

Solving the above relation gives the fourth order algebraic equation [3],

$$C_{H^+} + \frac{C_{Bo}}{\left(C_{H^+} + K_b\right)}C_{H^+} - \frac{C_{Ao}K_a}{\left(C_{H^+} + K_a\right)} + \frac{C_{Na^+bath}}{C_{H^+bath}}C_{H^+} - C_{Cl^-bath}\frac{C_{H^+bath}}{C_{H^+}} - \frac{K_w}{C_{H^+}} = 0$$

$$\left(C_{H^+}\right)^2 + \frac{C_{Bo}}{\left(C_{H^+} + K_b\right)}\left(C_{H^+}\right)^2 - \frac{C_{Ao}K_a}{\left(C_{H^+} + K_a\right)}C_{H^+} + \frac{C_{Na^+bath}}{C_{H^+bath}}\left(C_{H^+}\right)^2 - C_{Cl^-bath}C_{H^+bath} - K_w = 0$$

$$\left(C_{H^+}\right)^2 + \frac{C_{Bo}}{\left(C_{H^+} + K_b\right)}\left(C_{H^+}\right)^2 - \frac{C_{Ao}K_a}{\left(C_{H^+} + K_a\right)}C_{H^+} + \frac{C_{Na^+bath}}{C_{H^+bath}}\left(C_{H^+}\right)^2 - C_{H^+bath}\left(C_{Cl^-bath} - C_{OH^-bath}\right) = 0$$

$$\left(1+\frac{C_{Na^+bath}}{C_{H^+bath}}\right)\left(C_{H^+}\right)^2+\frac{C_{Bo}}{\left(C_{H^+}+K_b\right)}\left(C_{H^+}\right)^2-\frac{C_{Ao}K_a}{\left(C_{H^+}+K_a\right)}C_{H^+}-\left(C_{H^+bath}\right)^2\left(1+\frac{C_{Na^+bath}}{C_{H^+bath}}\right)=0$$

$$\left(C_{H^+}\right)^2+\frac{1}{\left(C_{H^+}+K_b\right)}\frac{C_{Bo}}{\left(1+C_{Na^+bath}/C_{H^+bath}\right)}\left(C_{H^+}\right)^2-\frac{1}{\left(C_{H^+}+K_a\right)}\frac{C_{Ao}K_a}{\left(1+C_{Na^+bath}/C_{H^+bath}\right)}C_{H^+}-$$
$$\left(C_{H^+bath}\right)^2=0$$

$$\left(C_{H^+}\right)^3+K_b\left(C_{H^+}\right)^2+\frac{C_{Bo}}{\left(1+C_{Na^+bath}/C_{H^+bath}\right)}\left(C_{H^+}\right)^2-$$
$$\frac{1}{\left(C_{H^+}+K_a\right)}\frac{C_{Ao}K_a}{\left(1+C_{Na^+bath}/C_{H^+bath}\right)}\left(C_{H^+}\right)^2-\frac{1}{\left(C_{H^+}+K_a\right)}\frac{C_{Ao}K_aK_b}{\left(1+C_{Na^+bath}/C_{H^+bath}\right)}C_{H^+}-$$
$$\left(C_{H^+bath}\right)^2C_{H^+}-K_b\left(C_{H^+bath}\right)^2=0$$

$$\left(C_{H^+}\right)^4+K_a\left(C_{H^+}\right)^3+K_b\left(C_{H^+}\right)^3+K_aK_b\left(C_{H^+}\right)^2+$$
$$\frac{C_{Bo}}{\left(1+C_{Na^+bath}/C_{H^+bath}\right)}\left(C_{H^+}\right)^3+\frac{K_aC_{Bo}}{\left(1+C_{Na^+bath}/C_{H^+bath}\right)}\left(C_{H^+}\right)^2-$$
$$\frac{C_{Ao}K_a}{\left(1+C_{Na^+bath}/C_{H^+bath}\right)}\left(C_{H^+}\right)^2-\frac{C_{Ao}K_aK_b}{\left(1+C_{Na^+bath}/C_{H^+bath}\right)}C_{H^+}-$$
$$\left(C_{H^+bath}\right)^2\left(C_{H^+}\right)^2-K_a\left(C_{H^+bath}\right)^2C_{H^+}-K_b\left(C_{H^+bath}\right)^2C_{H^+}-K_aK_b\left(C_{H^+bath}\right)^2=0$$

$$\left(C_{H^+}\right)^4 + \left\{K_a + K_b + \frac{C_{Bo}}{\left(1 + C_{Na^+bath} / C_{H^+bath}\right)}\right\}\left(C_{H^+}\right)^3 +$$
$$\left\{K_a K_b - \left(C_{H^+bath}\right)^2 + \frac{K_a\left(C_{Bo} - C_{Ao}\right)}{\left(1 + C_{Na^+bath} / C_{H^+bath}\right)}\right\}\left(C_{H^+}\right)^2 -$$
$$\left\{\left(K_a + K_b\right)\left(C_{H^+bath}\right)^2 + \frac{K_a K_b C_{Ao}}{\left(1 + C_{Na^+bath} / C_{H^+bath}\right)}\right\}C_{H^+} - K_a K_b\left(C_{H^+bath}\right)^2 = 0$$

The first derivative of this polynomial expression is

$$4\left(C_{H^+}\right)^3 + 3\left\{K_a + K_b + \frac{C_{Bo}}{\left(1 + C_{Na^+bath} / C_{H^+bath}\right)}\right\}\left(C_{H^+}\right)^2 +$$
$$2\left\{K_a K_b - \left(C_{H^+bath}\right)^2 + \frac{K_a\left(C_{Bo} - C_{Ao}\right)}{\left(1 + C_{Na^+bath} / C_{H^+bath}\right)}\right\}C_{H^+} -$$
$$\left\{\left(K_a + K_b\right)\left(C_{H^+bath}\right)^2 + \frac{K_a K_b C_{Ao}}{\left(1 + C_{Na^+bath} / C_{H^+bath}\right)}\right\} = 0$$

CONVERSION OF PIXEL TO MICRON IN THE IMAGES USED

Inner Diameter of a 100 micropipette = 165 pixels = 121.3228 microns

136 Pixel Value = 100 Microns

1 Pixel Value = 0.73529 Microns

MATLAB PROGRAM

```
clear all;      % Remove any previously defined variables
clc;            % Clear the command console

fileinfo = aviinfo('bachema_0001.avi');
nFrames = fileinfo.NumFrames
mov = aviread('bachema_0001.avi'); % Read in the avi file

% Show movie before processing
movie(mov,1);

%nFrames = 3;
for n = 1:nFrames
    [I,map] = frame2im(mov(n));
    %figure, imshow(I);title('First frame of bacteria movie')
    x = RGB2GRAY(I);
    se1=strel('disk',10);
    se2=strel('disk',4);
    Itop = imtophat(x, se1);
    Ibot = imbothat(x, se2);
    Ienhance = imsubtract(imadd(Itop, x), Ibot);
    H = fspecial('unsharp');
    sharpened = imfilter(Ienhance,H);
    I3 = imadjust(sharpened,stretchlim(sharpened),[0 1]);
    L = medfilt2(I3,[3 3]);
    q=edge(L,'sobel');
    se90 = strel('line', 3, 90);
    se0 = strel('line', 3, 0);
    BWsdil = imdilate(q, [se90 se0]);
    rr=bwfill(BWsdil,'holes');
    r = medfilt2(rr,[3 3]);
    bw2 = bwareaopen(r, 40, 26);
    se = strel('line',3,90);
    bw3 = imclose(bw2,se);
    op=imopen(bw3,se);
    bw4 = bwareaopen(op, 40, 26);
    [labeled,numObjects] = bwlabeln(bw4,8);% Label components.
    RGB_label = label2rgb(labeled, @spring, 'c', 'shuffle');
    %figure,imshow(RGB_label);title('Connected objects');
    num = numObjects;
%     imshow(X, map,'InitialMagnification','fit');
    imwrite(bw4,'an.bmp','bmp');
    [an,map] = imread('an.bmp');
    if n > 1
        a  = cat(4,ap,an);
        ap = a;
    else
        a  = an;
        ap = an;
    end
    mov(n) = getframe;
    close;
    n
```

```
end

% Show movie after processing
movie(mov,1);
mov2=immovie(a,map);
movie(mov2,1,2);

%figure,imshow(a(:, :, :, 1) );

% Determine the total number of frames acquired.
%nFrames = size(a,4)

% Crop the first frame.
first_frame1 = a(:,:,:,1);
figure,imshow(first_frame1);
rect1=[380,220,50,50];
first_region1 = imcrop(first_frame1,rect1);
figure,imshow(first_region1);

% Crop all the frames
for count = 1:nFrames
 frame_regions1(:,:,:,count) = imcrop(a(:,:,:,count),rect1);
 pause(0.2)
end
mov1=immovie(frame_regions1,map);
figure,movie(mov1,1,30);  % Play the move once at 5 frames per second

% Initialize an array to contain the segmented bac frames.
i=1;
for count = 1:nFrames

    fr1 = frame_regions1(:,:,:,count);
    %figure,imshow(fr),title('single bac');
    pause(0.2)
    % Labeling components.
    [labeled,numObjects1] = bwlabeln(fr1,8);
    if(numObjects1~=0)
        %break;
        %fr1 = frame_regions1(:,:,:,count+1);
        %figure,imshow(fr),title('no bac ');
        %pause(0.2)
        %[labeled,numObjects1] = bwlabeln(fr1,8);
        %  else
        %end
    %pause(0.2)


    property1 = regionprops(labeled,'Centroid');
    bac_centers1 = property1(1).Centroid;
    bac_centers1
    %finding the x and y coordiantes for BAC1
    x1(i)=bac_centers1(:,1);
    y1(i)=bac_centers1(:,2);

    i=i+1;
```

```
    time=i;
else
%     x1(i)=0;
%     y1(i)=0;
%     i=i+1;
%
    continue;
%     if i>nFrames
%         break
%     end
end
end

%Plot the x-y coordinates
figure, plot(x1,y1,'--rs'), axis ij, axis equal, hold on;
xlabel('x1');
ylabel('y1');
title('first bac centers');

%Save the time and x-y coordinates to a text file
t = 1:1:time-1;
fid = fopen('xyz.txt','w');
fprintf(fid,'Time (sec)\tX\tY\n');
for n = 1:i-1
    fprintf(fid,'%6.2f\t%12.8f\t%12.8f\n',t(n),x1(n),y1(n));
end
fclose(fid);
```

APPENDIX 3: FIGURES

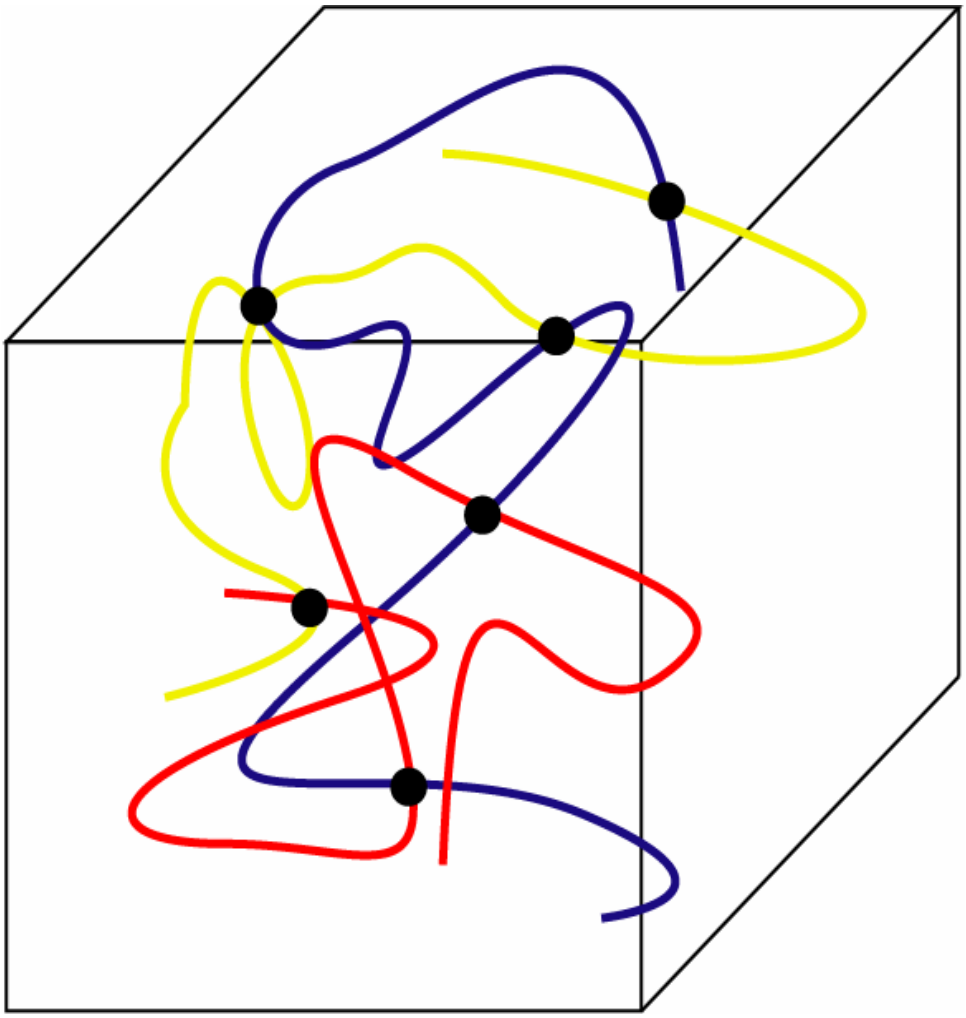

Figure A3-1. 3-dimentional model of hydrogel

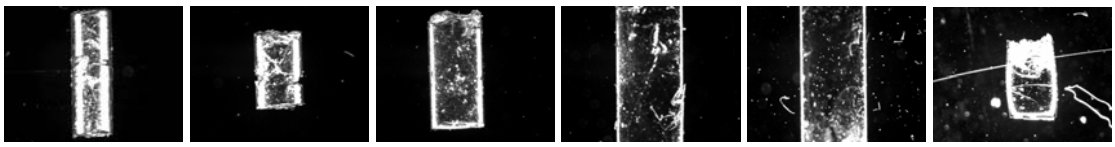

Figure A3-2. Microscopic images of balanced polyampholyte hydrogel with charges 0, 40, 80, 120, 160, 200 mM taken on Jan30.

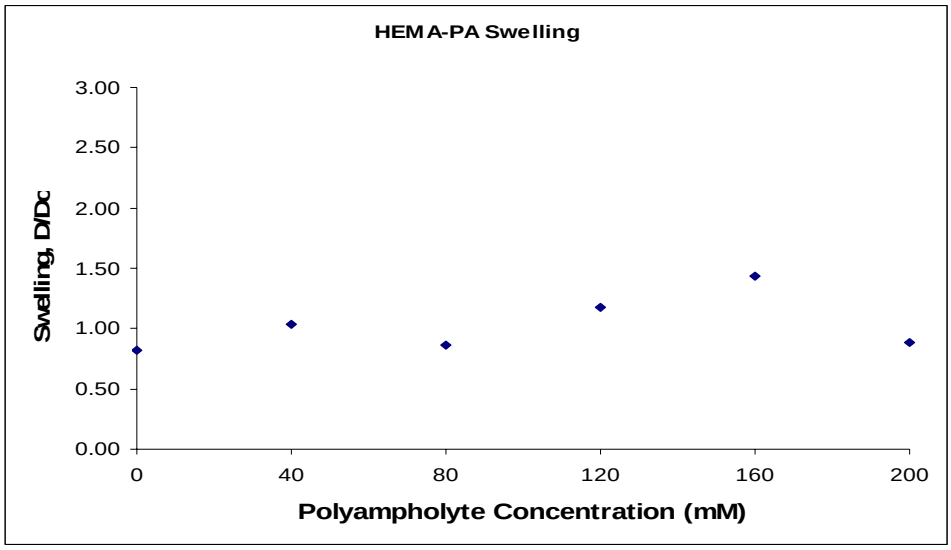

Figure A3-3. Graph has been plotted with the initial swelling measurement data for balanced polyampholyte hydrogel with charges 0, 40, 80, 120, 160, 200 mM taken on Jan 30 after washed with DI water.

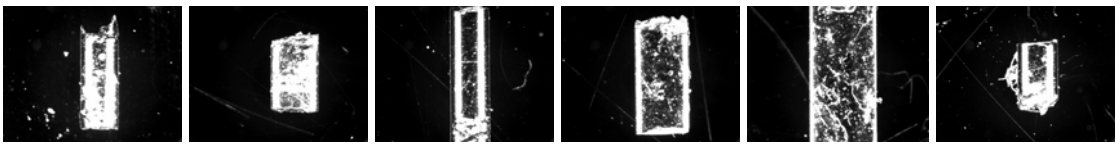

Figure A3-4. Microscopic images of balanced polyampholyte hydrogel with charges 0, 40, 80, 120, 160, 200 mM taken on Feb 11.

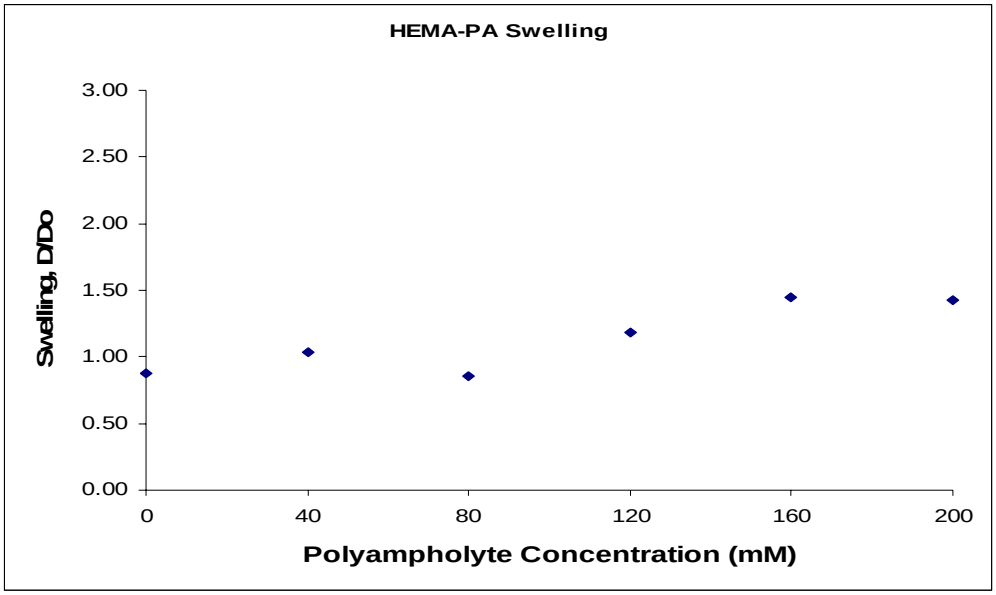

Figure A3-5. Graph has been plotted with the swelling measurement data taken until Feb 11 for balanced polyampholyte hydrogel with charges 0, 40, 80, 120, 160, 200 mM.

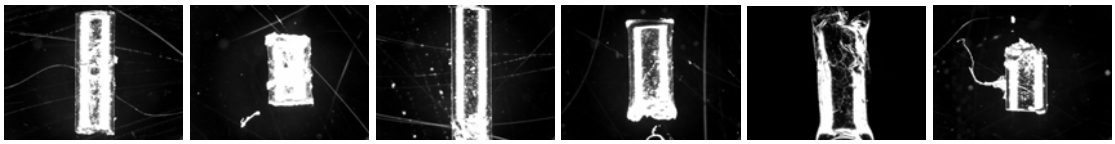

Figure A3-6. Microscopic images of balanced polyampholyte hydrogel with charges 0, 40, 80,120,160,200 mM taken on Feb 13.

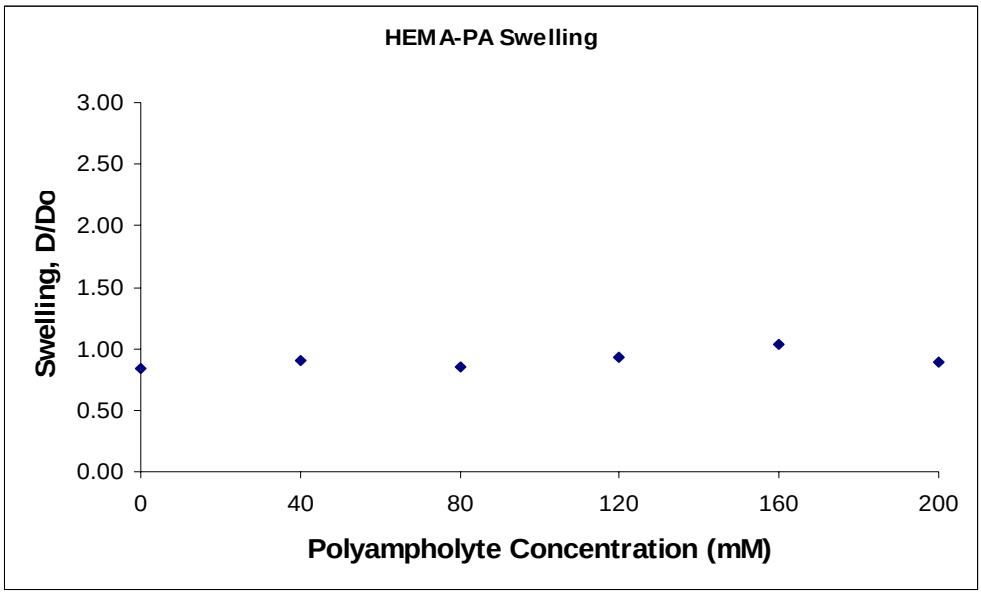

Figure A3-7. Graph has been plotted with the swelling measurement data taken on 13th (after gels in 1.54mM NACL bath) for balanced polyampholyte hydrogel with charges 0, 40, 80, 120, 160, 200 mM.

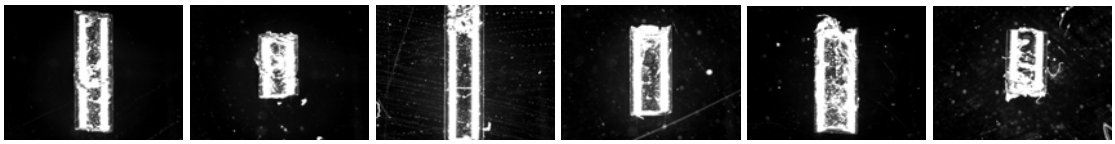

Figure A3-8. Microscopic images of balanced polyampholyte hydrogel with charges 0, 40, 80,120,160,200 mM taken on Feb 16.

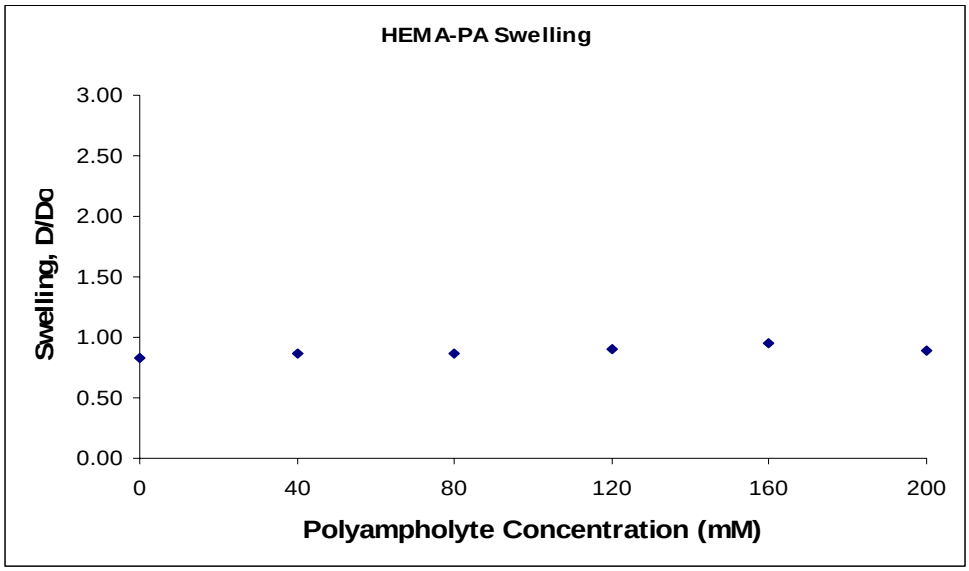

Figure A3-9. Graph has been plotted with the swelling measurement data taken until 16th (gels are still in 1.54mM NACL bath) for balanced polyampholyte hydrogel with charges 0, 40, 80, 120, 160, 200 mM.

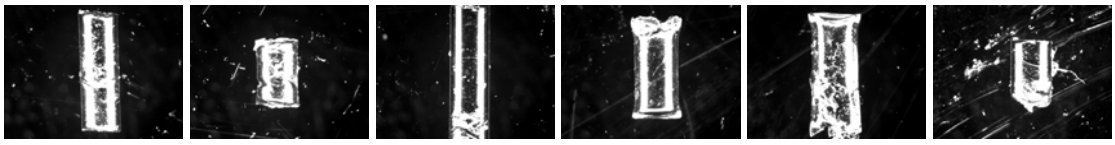

Figure A3-10. Microscopic images of balanced polyampholyte hydrogel with charges 0, 40, 80,120,160,200 mM taken on Feb 23.

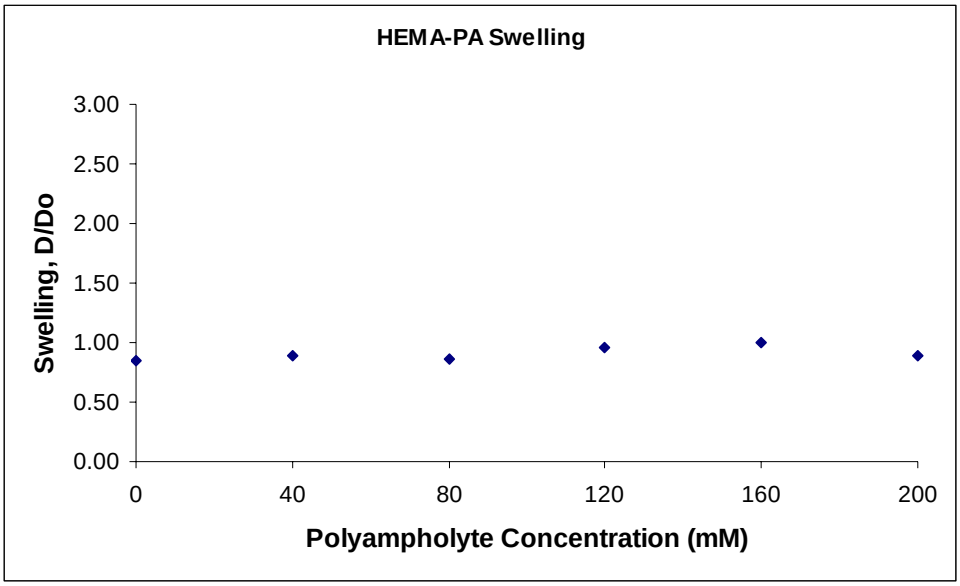

Figure A3-11. Graph has been plotted with the swelling measurement data taken until 23rd (gels are now being washed in PBS bath) for balanced polyampholyte hydrogel with charges 0, 40, 80, 120, 160, 200 mM.

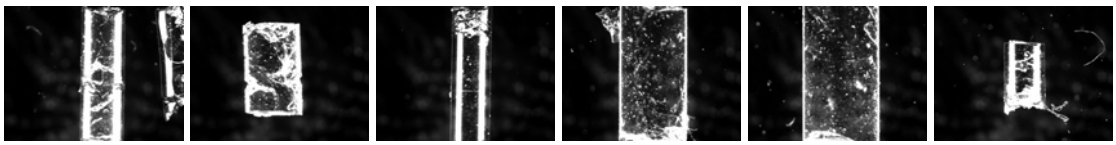

Figure A3-12. Microscopic images of balanced polyampholyte hydrogel with charges 0, 40, 80,120,160,200 mM taken on Feb 27.

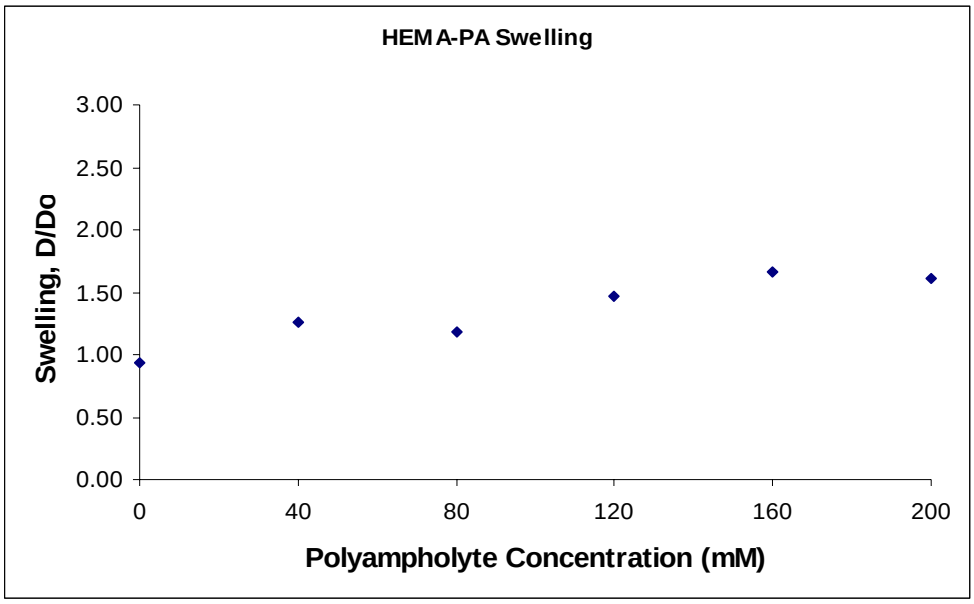

Figure A3-13. Graph has been plotted with the swelling measurement data taken until 27th (gels are now washed in DI bath after being washed with PBS) for balanced polyampholyte hydrogel with charges 0, 40, 80, 120, 160, 200 mM.

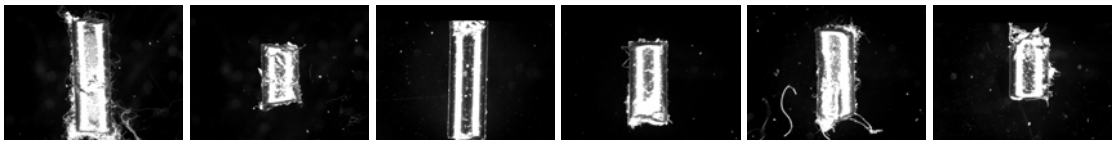

Figure A3-14. Microscopic images of balanced polyampholyte hydrogel with charges 0, 40, 80,120,160,200 mM taken on Apr 15.

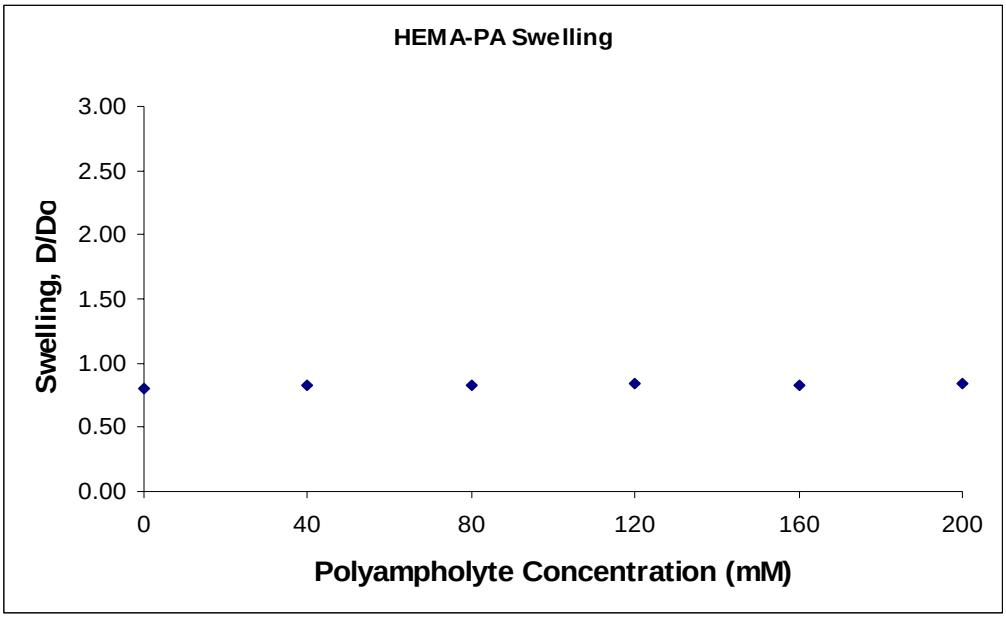

Figure A3-15. Graph has been plotted with the swelling measurement data taken on April 15th (gels are now washed in 1.54 M NACL) for balanced polyampholyte hydrogel with charges 0, 40, 80, 120, 160, 200 mM.

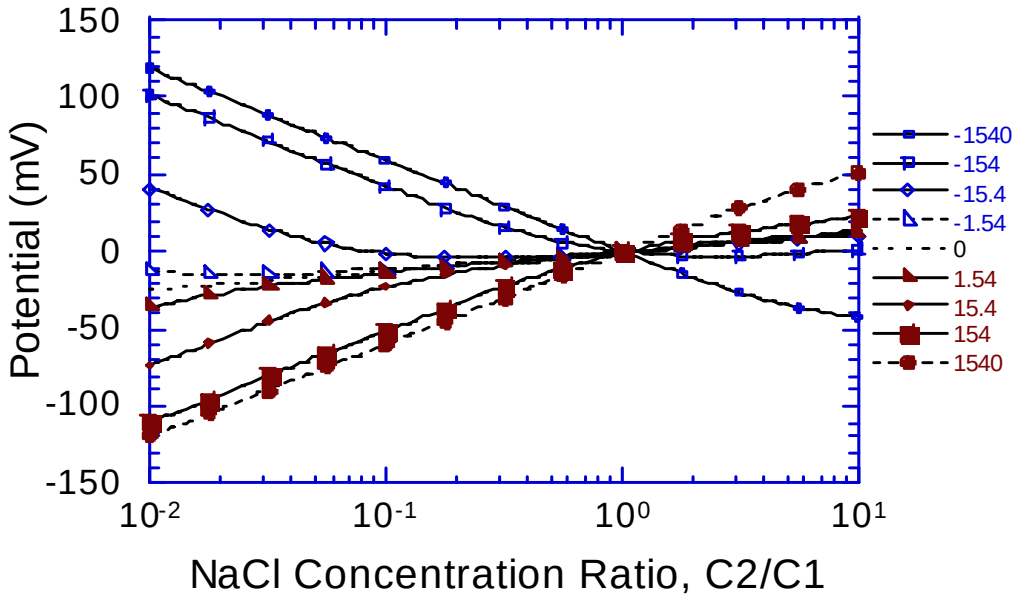

Figure A3-16. Hydrogel diffusion potential simulations for negative and positive hydrogels.

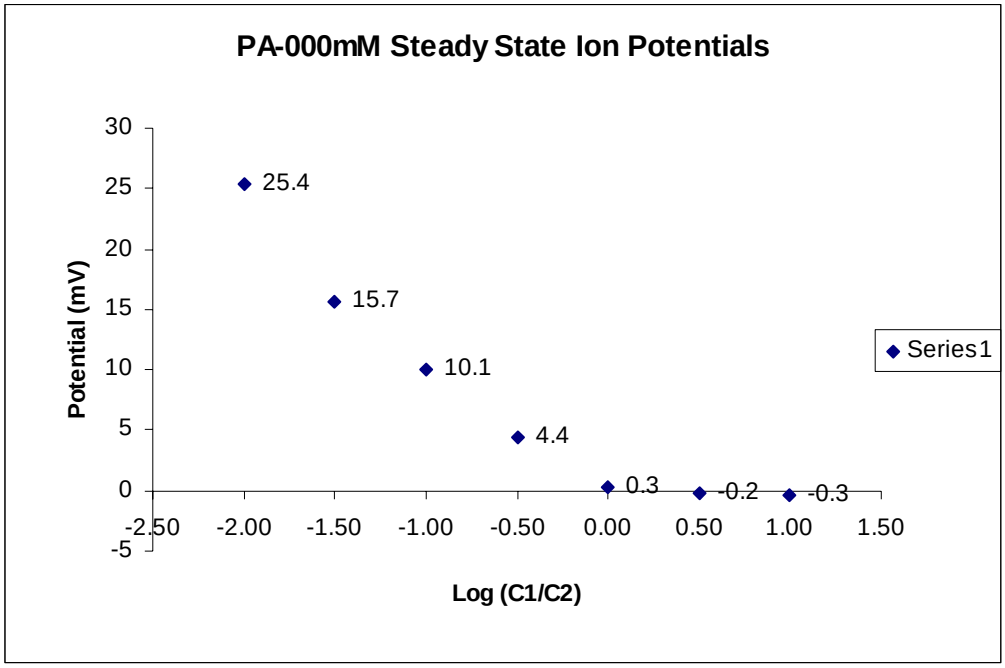

Figure A3-17. Graph showing the diffusion potential measurement of balanced polyampholyte hydrogel with the 0mM charge.

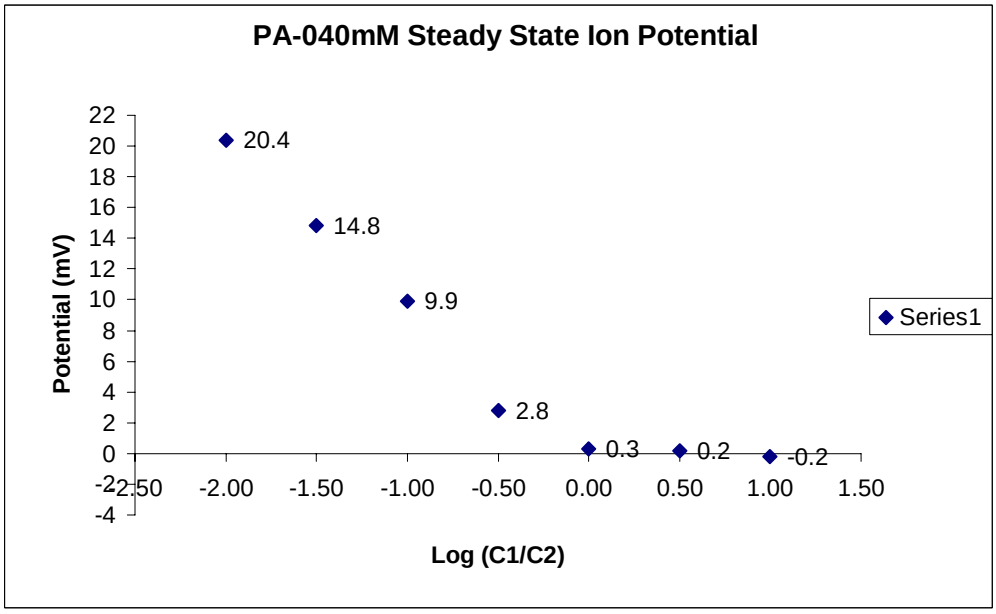

Figure A3-18. Graph showing the diffusion potential measurement of balanced polyampholyte hydrogel with the 40mM charge.

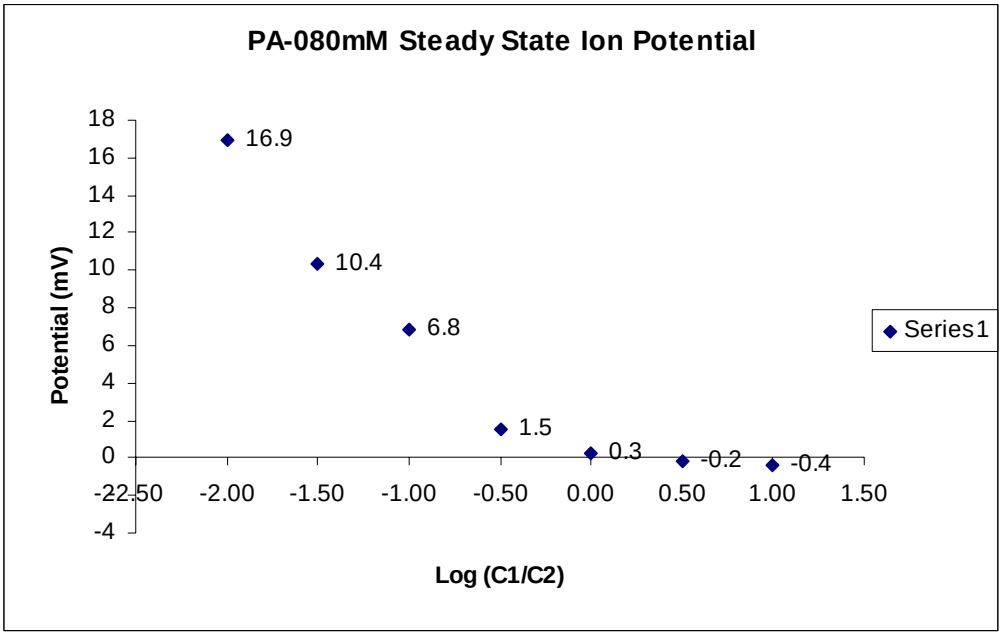

Figure A3-19. Graph showing the diffusion potential measurement of balanced polyampholyte hydrogel with the 80mM charge.

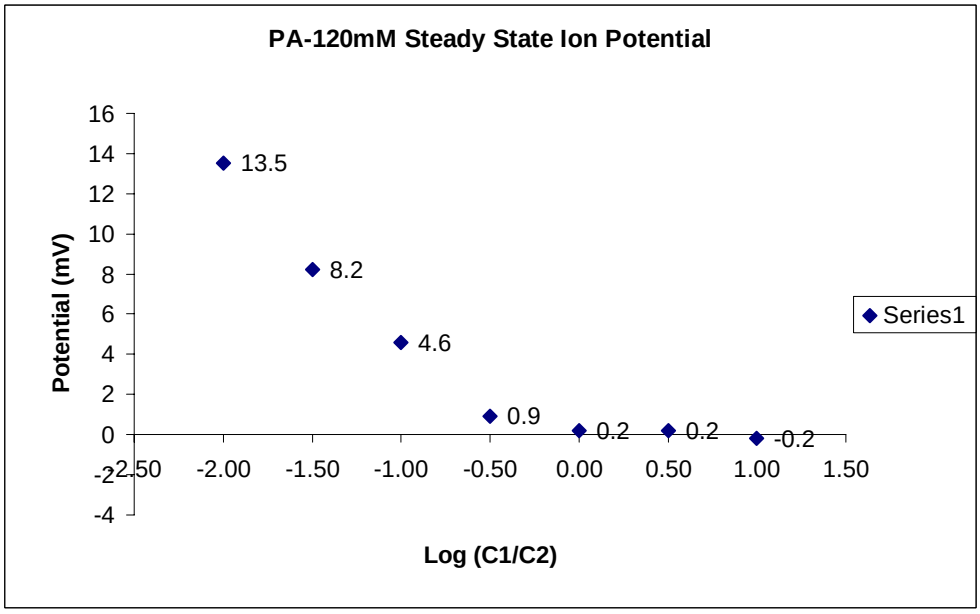

Figure A3-20. Graph showing the diffusion potential measurement of balanced polyampholyte hydrogel with the 120mM charge.

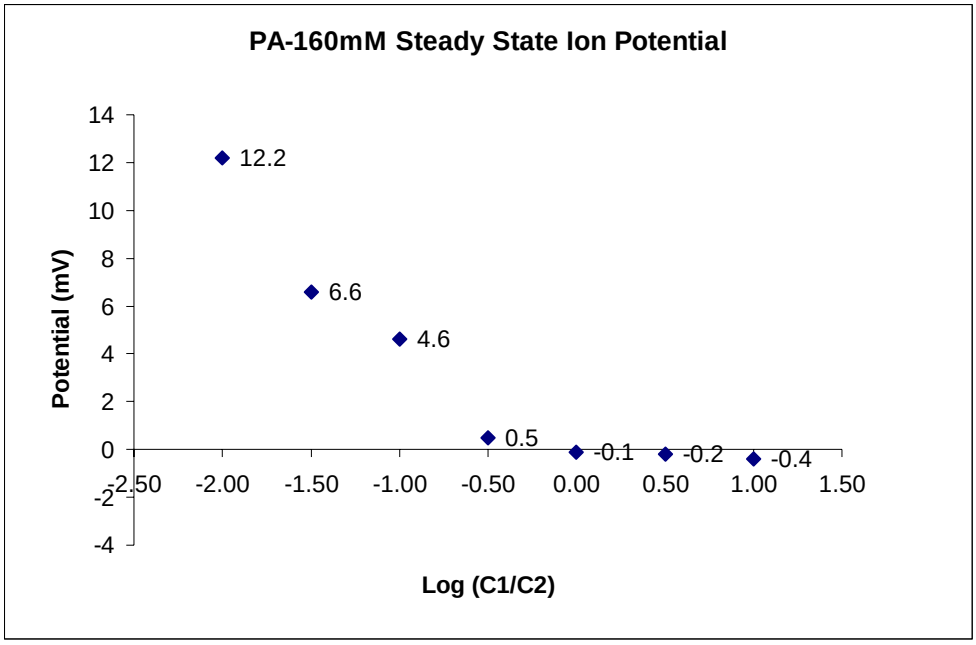

Figure A3-21. Graph showing the diffusion potential measurement of balanced polyampholyte hydrogel with the 160mM charge.

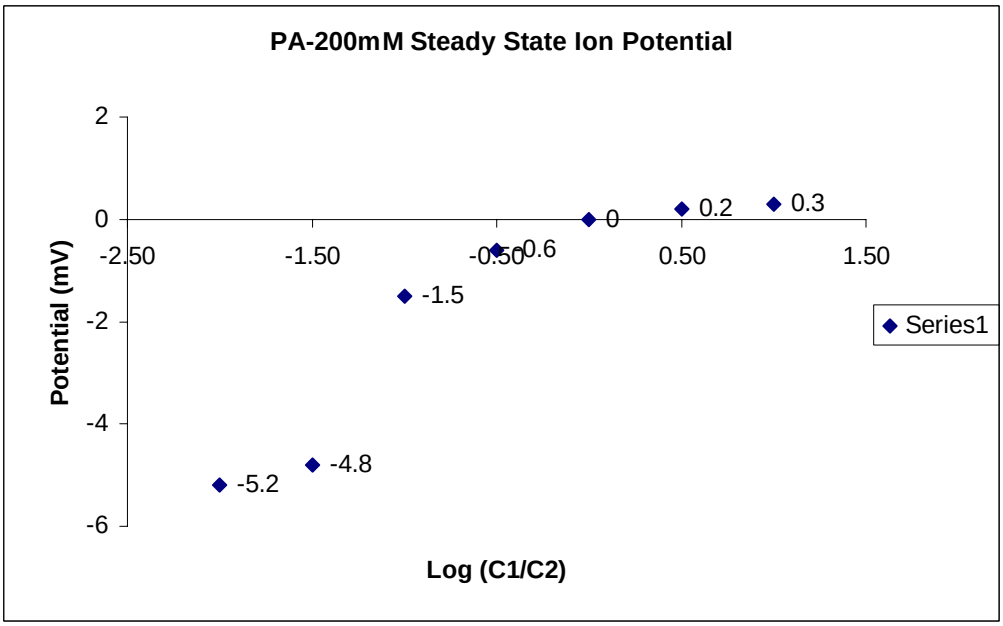

Figure A3-22. Graph showing the diffusion potential measurement of balanced polyampholyte hydrogel with the 200mM charge.

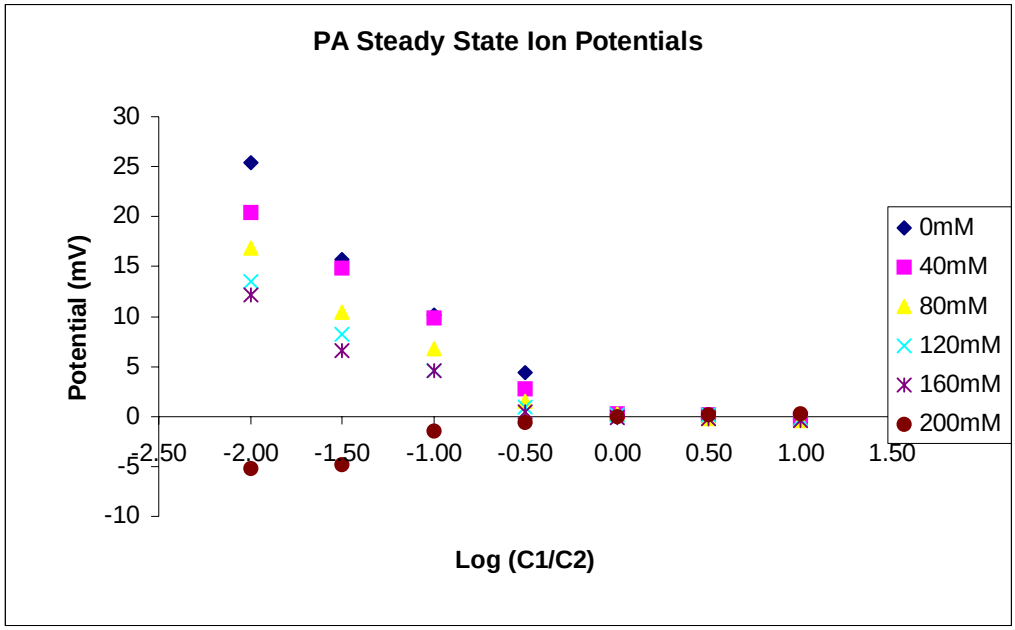

Figure A3-23. Graph showing the diffusion potential measurement of balanced polyampholyte hydrogel with charges 0, 40, 80, 120, 160, 200 mM.

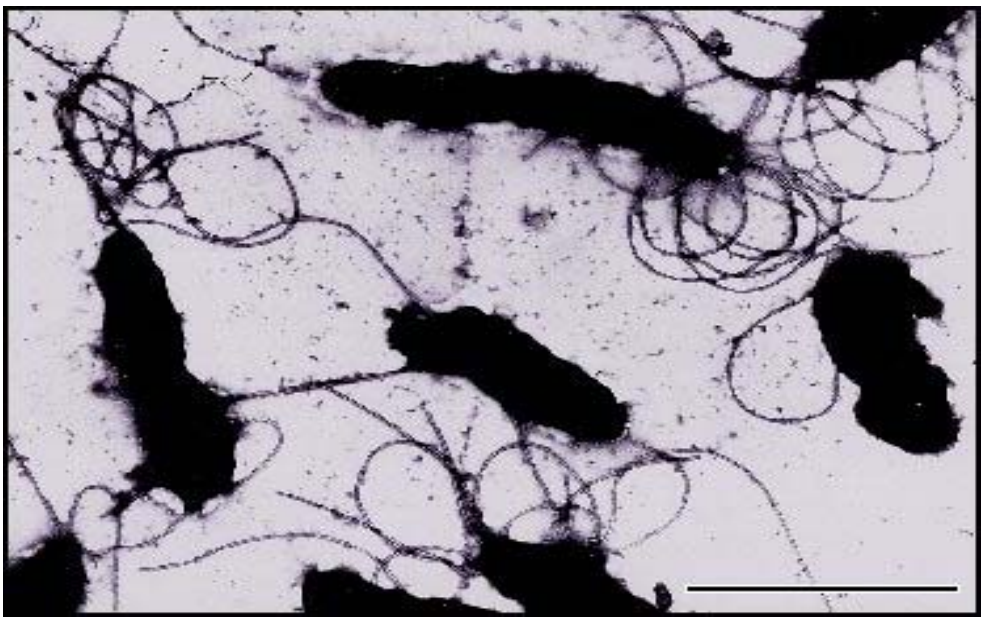

Figure A3-24. Bacteria Pseudomonas fluorescens 5RL with Scale 1 µ taken from a Transmission electron microscopy (TEM).

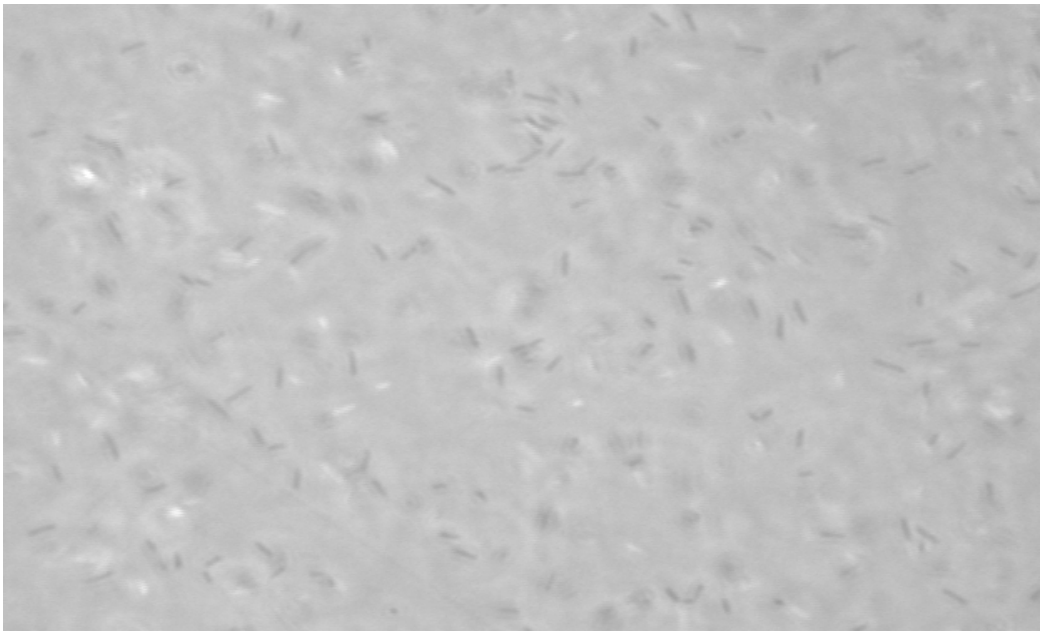

Figure A3-25. Sample Microscopic image of bacteria Pseudomonas fluorescens 5RL over a balanced polyampholyte hydrogel surface.

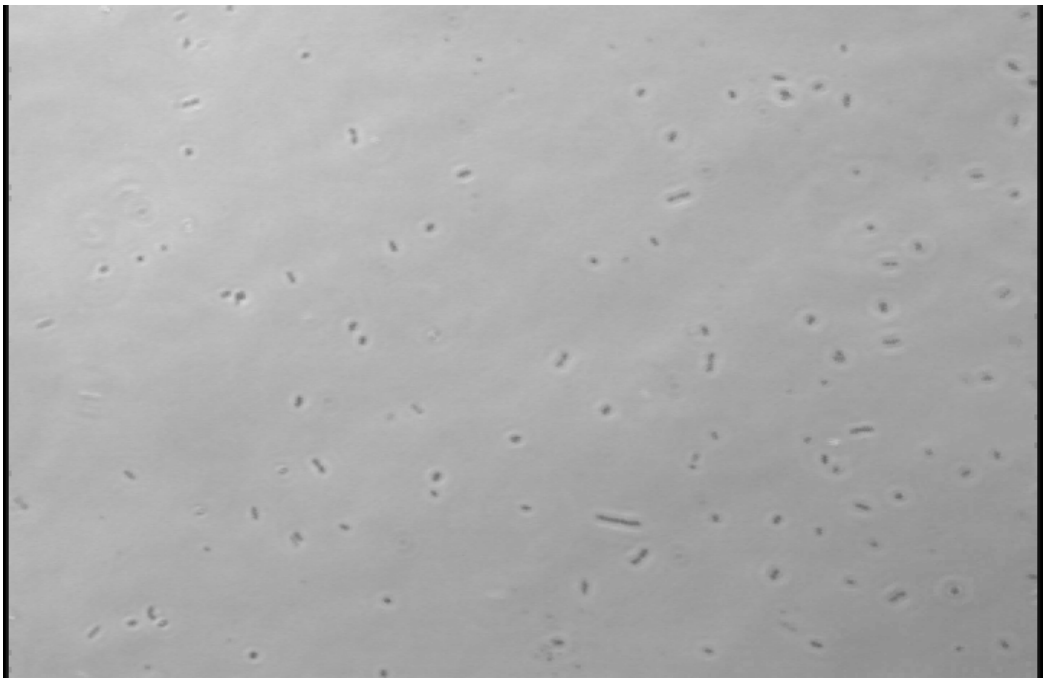

Figure A3-26. A single frame of image taken from the AVI file which is going to be subjected to various image processing techniques.

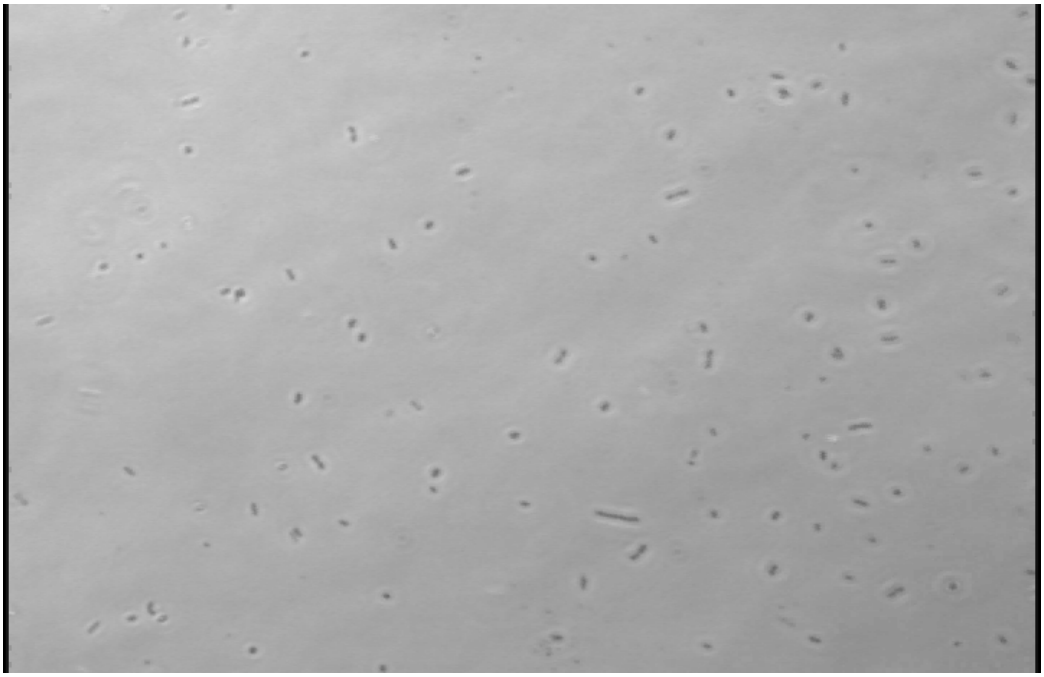

Figure A3-27. Image obtained as a result of using Top-hat and Bottom-hat filtering

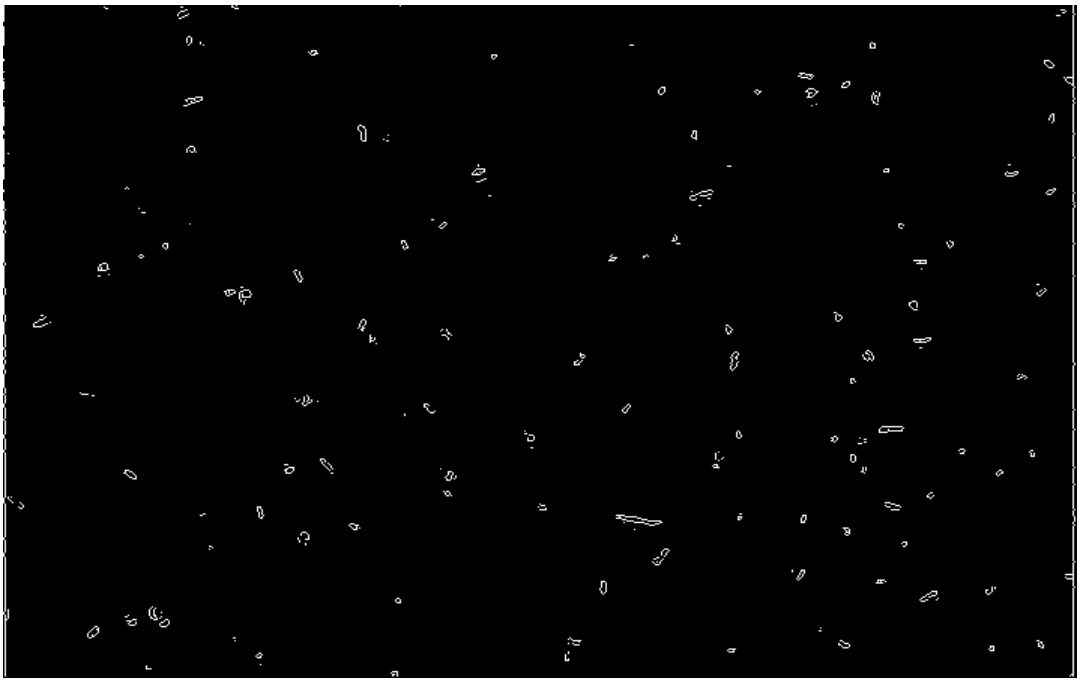

Figure A3-28. Image obtained after the application of Edge detection technique.

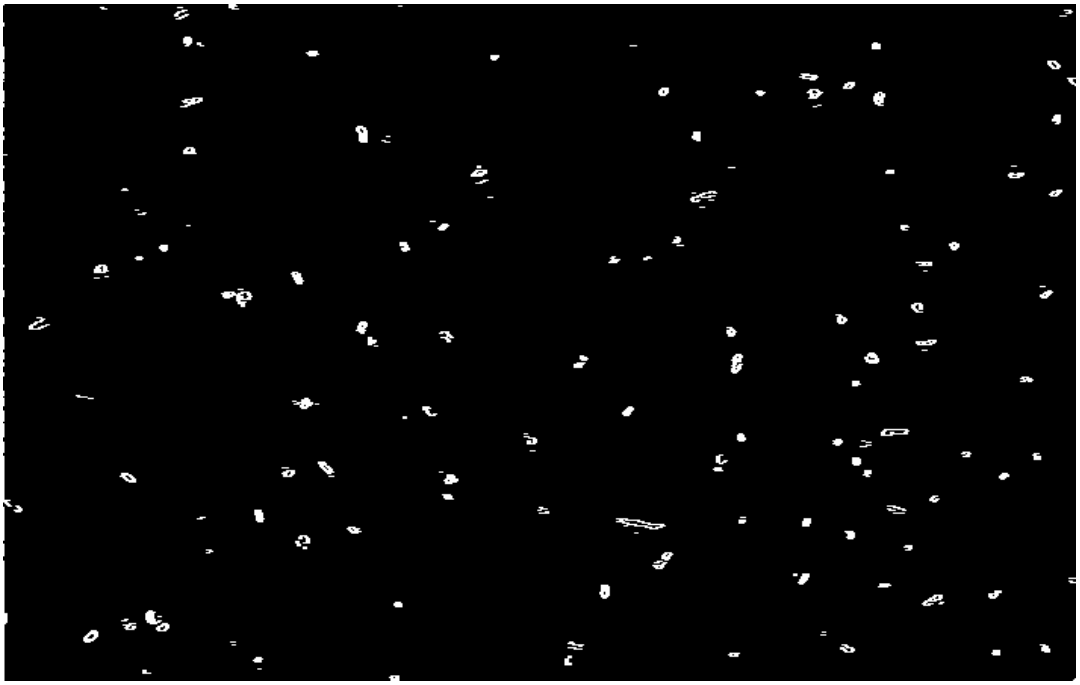

Figure A3-29. Image after the Dilation method which fills the holes formed during the edge detection method.

Figure A3-30. Image applying Median filter to remove the noises and small particle other than the bacteria.

Figure A3-31. Image after the morphological Closing which carefully widen the bacteria area to join the uncovered holes.

Figure A3-32. Image after the morphological Opening which carefully sharpens the bacteria area.

Figure A3-33. The final Image clearly showing the bacteria in the white spot

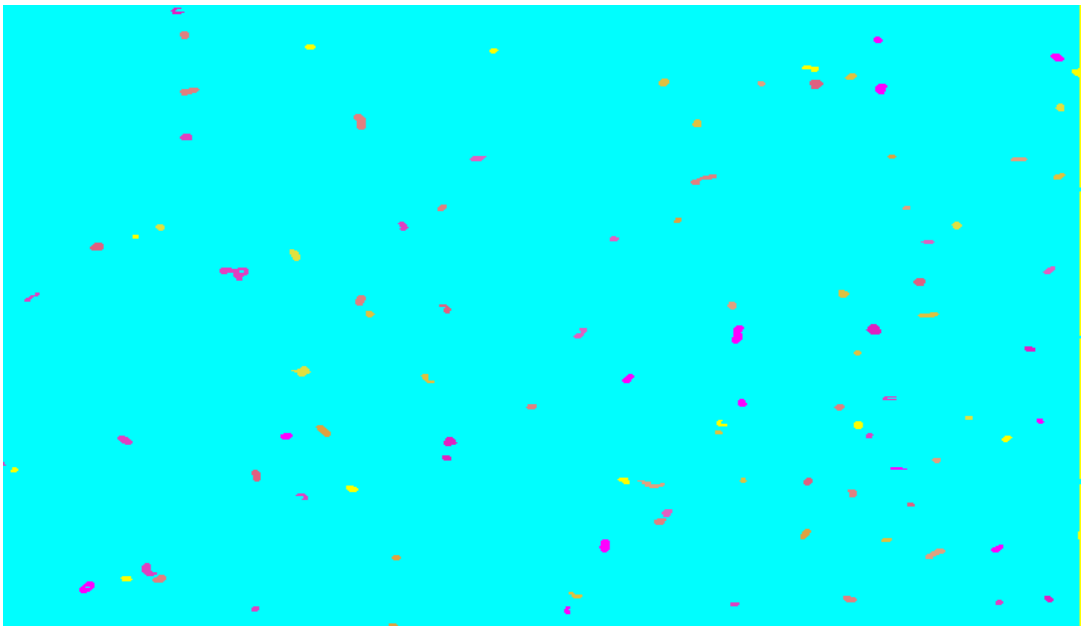

Figure A3-34. Image showing the connected objects (bacteria) in different color to identify the individual bacteria from the neighboring bacteria.

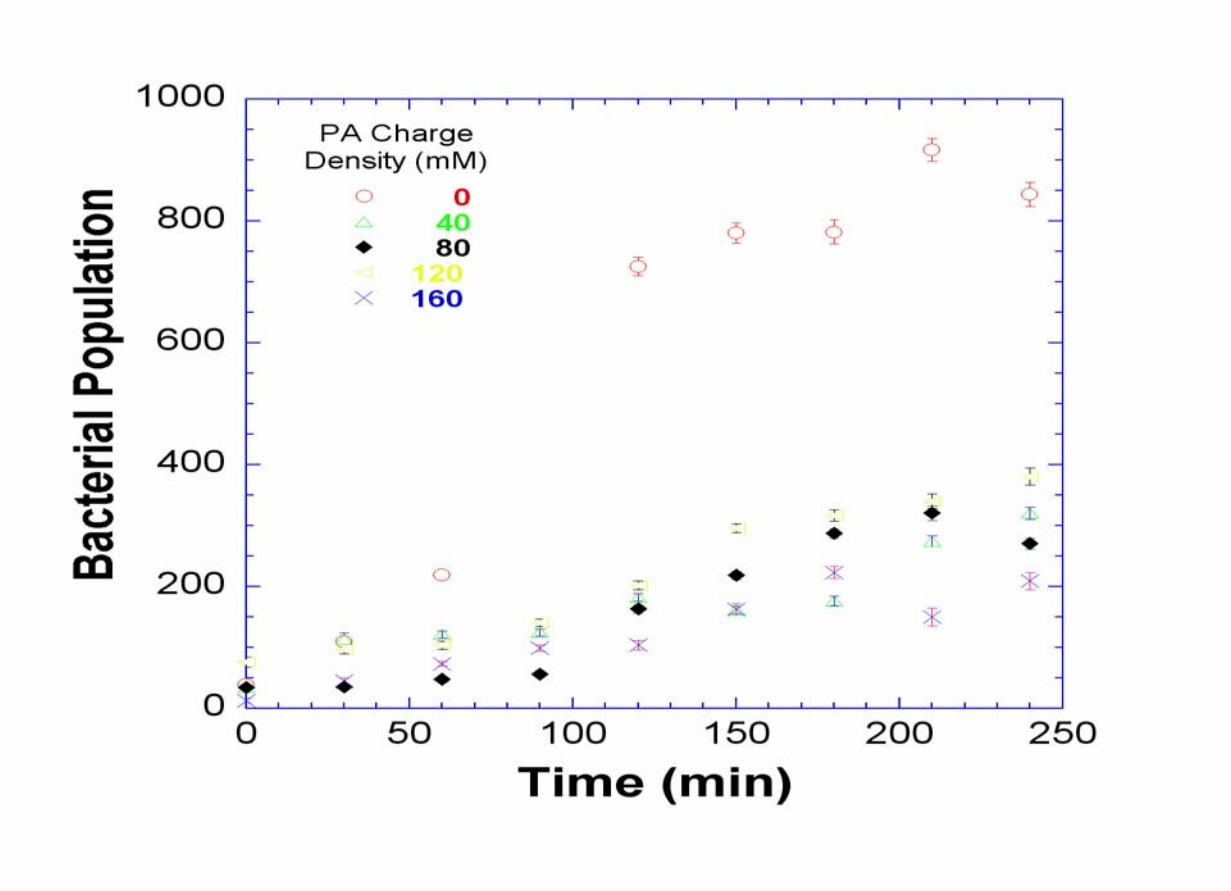

Figure A3-35. Bacterial growth curves on charge balanced polyampholyte hydrogels as a function of time. Population per 61.536 X 10^{3} Micron ^{2}

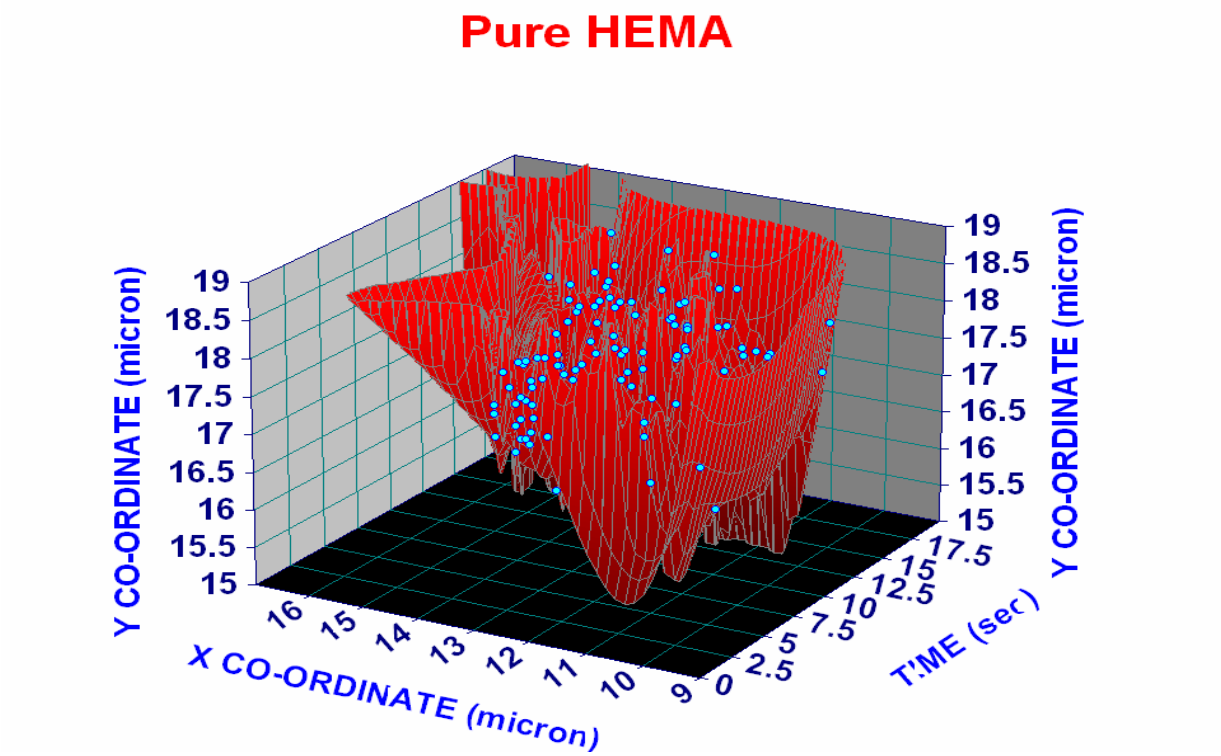

Figure A3-36. Bacterial micro motion (in microns) on a neutral HEMA hydrogel with respect to time (in seconds).

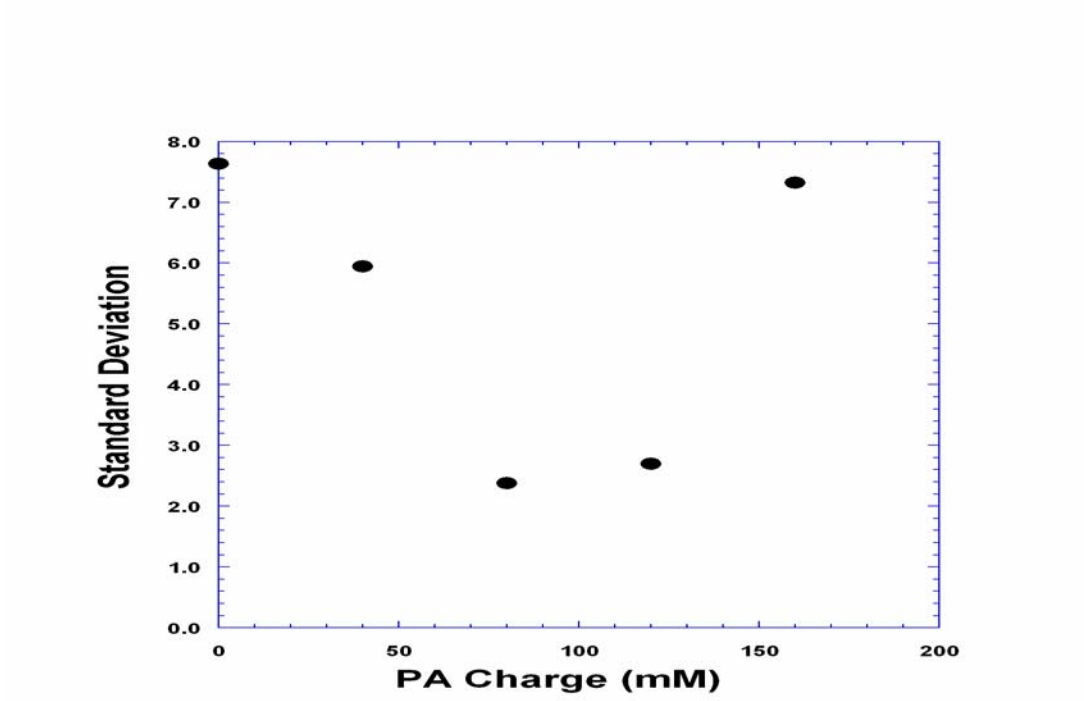

Figure A3-37. The Standard deviation (in Microns) of 60 seconds of bacterial micro motion as a function of balanced polyampholyte charge density (in mM)

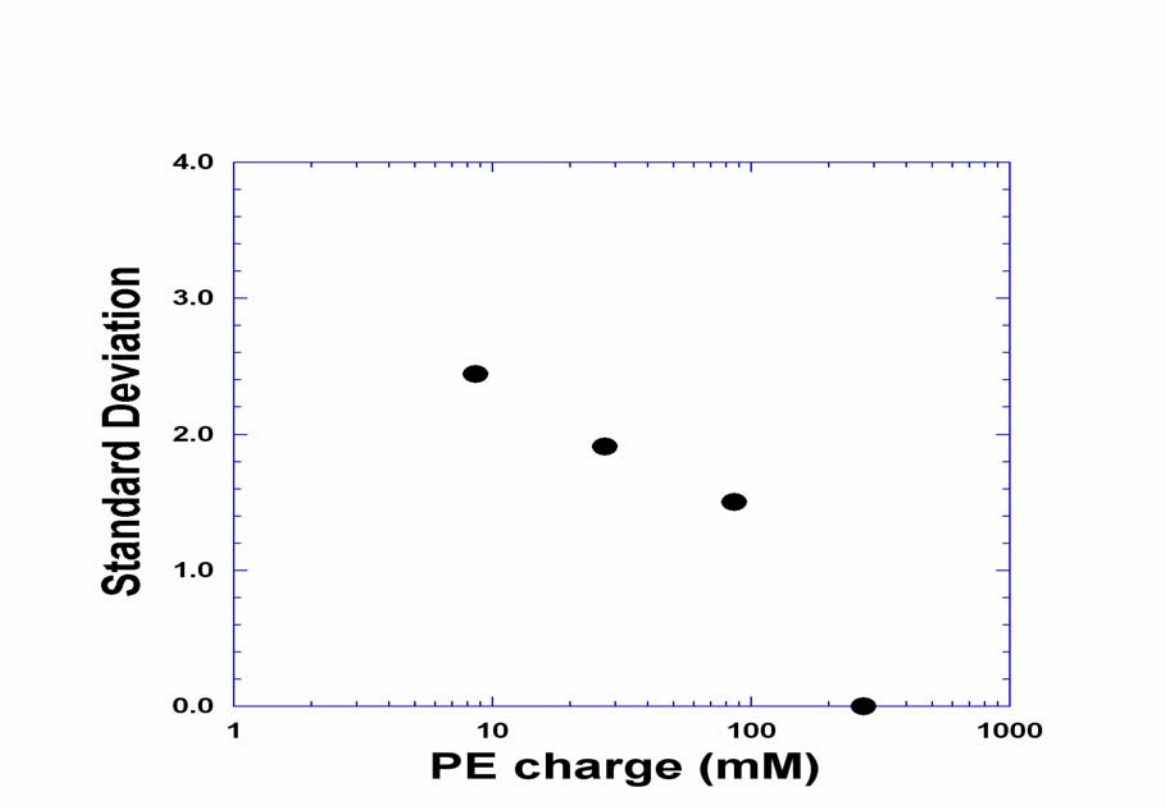

Figure A3-38. The Standard deviation (in Microns) of bacterial micro motion on positively charged hydrogel showing decreasing micro motion with increasing positive charge density (in mM)

VITA:

Ram Pratap Gangadharan was born November the 18th, 1978 in Chennai, INDIA. He graduated from University Of Madras, India with Electrical and Electronics Engineering as major. He came to the University of Tennessee, Knoxville to purse a M.S. in Engineering Science with a Biomedical emphasis. Ram Pratap is currently looking for a position in Biomedical Engineering.